(2)

QUARTERLY REPORT FOR ALE PROJECT JUNE 1992

Contract # N00014-91-C-0080

Submitted by

S. M. Gates, F. J. Himpsel, S. S. Iyer, F. R. Mc Feely,
T. O. Sedgwick, T. P. Smith, III, and R. Tromp

IBM Research Division
T. J. Watson Research Center
Yorktown Heights, New York

IBM

ALE Quarterly Report

Progress in the IBM ALE project was made in several areas. Most of these results were reported at the 2nd Annual ALE Conference at Raleigh, NC in June 1992. We summarize the main results here and include details in the appendices.

1. Fundamental Surface Chemistry Studies

a. Study of H/Cl exchange chemistry on Si(100) using Si_2Cl_6 and Si_2H_6

A study of H/Cl exchange on Si(100) using Si_2H_6 and Si_2Cl_6 has been conducted and is described in Appendix A. The following conclusions have been reached:

1. The stable, commercially available molecules Si_2H_6 and Si_2Cl_6 form a viable pair of reactant molecules for Si growth using cycles of alternating gas exposures in the T range 450-500°C.
2. This scheme is not truly self-limiting but it does retain some of the desirable features of true ALE growth.
3. Simple thermal desorption of HCl and H_2 products explains the observed T dependance of this exchange chemistry. Formation of the H-Cl bond in the HCl product desorption step does not appear to "assist" the growth process by contributing any energy to the Si surface.
4. Doping the surface with BH_x groups or with B atoms lowers the T for H/Cl exchange, by weakening both the Si-Cl and Si-H surface bonds.

b. A study of the dopants B, Ge and Sn on Si(100), and the prospects for using these as "elemental marker layers" for study of Si ALE

A study of dopant "marker layers" on Si(100) has been conducted and is described in Appendix B (Gates and Koleske; Appl. Phys. Lett., submitted). Submonolayer coverages of *B, Sn and* Ge are prepared on Si(100) surfaces, and characterized using time-of-flight Scattering and Recoiling Spectroscopy (TOF-SARS). The dopant "marks" the initial Si interface, and Si is grown on top of the "marked" surface, and is designated Si^*. *Attenuation* of the elemental B, Sn and Ge signals by Si^* is used to evaluate Si precursors for Atomic Layer Epitaxy (ALE), and compare the thermal stability of Si^*/B/Si(100), Si^*/Sn/Si(100) and Si^*/Ge/Si(100) structures. We find that boron "markers" are stable to higher T than Sn or Ge.

The dopants Sn and Ge tend to segregate (as is well known during MBE Si growth). We have proven that termination of the surface dangling bonds with H or Cl prevents Ge segregation, for temperatures below the H_2 or $GeCl_2$ desorption threshold. The Si^*/Sn/Si(100) and Si^*/Ge/Si(100) structures are only stable provided the Si^* surface is terminated with hydrogen or Cl. These 2 structures decompose below 450°C by dopant segregation to the surface when the surface dangling bonds are not terminated.

c. Work in Progress

At present, D. D. Koleske is evaluating the Si precursors SiH_3Cl, SiH_2Cl_2 and Si_2Cl_6 with the goal of choosing an optimum chlorosilane precursor. Kinetic studies of Cl and Br extraction by H atoms are intended, with the intention of providing evidence for/against an Eley-Rideal reaction mechanism. Further studies of elemental markers are also planned. At the present, S. M. Gates is growing thin Si layers using the Si_2Cl_6/Si_2H_6 process. Both Ge(100) and boron-marked Si (B/Si) substrates are used. TEM cross-sections are being used to evaluate thickness, conformality (thickness homogeneity) and epitaxial quality. LEED is used to follow epitaxy *in situ*.

2. Photoemission Study of ALE Mechanisms

a. Photoemission

High resolution, soft x-ray photoemission experiments were performed, which illustrate the chemical mechanisms involved in the chemisorption and subsequent reaction between Germanium tetrachloride ($GeCl_4$) and Silicon tetrachloride ($SiCl_4$) and Si(111) and Si(100) surfaces. At sufficiently low temperature, the chemisorption was found to be self-limiting. Exposures of the substrates to 25000 Langmuirs of $GeCl_4$ and $SiCl_4$ were completed as a function of the sample temperature from room temperature to 800°C. Ge 3d, Si 2p and Cl 2p core level photoemission spectra were obtained following each exposure. $GeCl_4$ chemisorbs dissociatively forming $GeCl_3$, $GeCl_2$, and GeCl species as well as elemental germanium bonding to Si. An exposure of the Si(111) substrate to $GeCl_4$ at 200 and 300°C results in the reduction of the higher germanium chlorides to trace amounts of GeCl. Above 300°C only elemental Ge remains bonded to the Si substrate. In contrast to that observed on the Si(111) surface, exposures of Si(100) to $GeCl_4$ at 200 and 300°C results in significant amounts of $GeCl_2$ and GeCl species. At higher temperatures we observe the loss of the $GeCl_2$ component, but trace amounts of GeCl remain on the surface until temperatures above 600°C are attained. The corresponding Si 2p spectra for the two surfaces show that at all temperatures up to 700°C, the decomposition of $GeCl_4$ promotes the formation of silicon monochloride surface species.

The reaction of $SiCl_4$ with Si(111) (See L.J. Whitman, S.A. Joyce, J.A. Yarmoff, F.R. McFeely and L.J. Terminello, Surf. Sci. 232, 297 (1990)) and Si(100) substrates showed that at all temperatures up to 700°C, $SiCl_4$ chemisorbs dissociatively forming silicon monochloride surface species. Trace amounts of silicon dichloride moieties are also observed between sample temperatures of 300 to 500°C. Si 2p spectra obtained following exposures of the samples to 800°C show that no Cl remains bonded to the Si(111) or Si(100) surfaces. In addition, Si(111) and Si(100) surfaces were exposed to $SiCl_4$ at 400°C. The reacted surfaces were exposed to atomic hydrogen to remove the passivating Cl from the surfaces.

b. Work in Progress

A project has been started to study the adsorption of diethylsilane on Si with surface-sensitive core level and valence spectroscopy. Preliminary results show two sharp, low-lying valence orbitals of diethylsilane adsorbed at room temperature that have not been observed previously. They are assigned to C-H bonds. We expect to use them for fingerprinting the desorption and/or decomposition of the ethyl groups during growth of Si at elevated temperature.

3. ALE Processes for Doping in Si-based Epitaxy

We describe the results of our initial investigations of doping through ALE-like reactions. For practical fabrication of even conventional devices such as bipolar transistors and FETs, we require a very precise control of the dose, and to some extent its location. Very often, the final profile of the dopant is determined by subsequent and required processing, (such as silicide formation). ALE processes find useful application here. We describe two potential applications for both n- and p-type dopants first in MBE and then in CVD.

In MBE growth, the surface coverage of Sb on a stationary Si surface saturates at about one monolayer. However, it does not saturate if a Si flux is co-incident It is thus possible to meter out Sb in Si using this process in units of 1 ML ($\simeq 10^{15}$ cm^{-2}) quite exactly. It is possible to use controlled desorption of Sb to control the Sb to as low as 0.01 ML, but that is not an ALE process. However, subsequent Si growth at even moderate temperatures, leads to Sb segregation and the profile is smeared in the growth direction. This problem can be alleviated through the use of amorphous Si deposition and Solid Phase Epitaxy.

We have also observed a similar effect in APCVD using AsH_3 with silicon growth from $SiCl_2H_2$ The experiments we performed were as follows: AsH_3 was injected into the reactor during growth interruptions. Whereas the temperature of the silicon growth was kept constant at 650°C, the AsH_3 flushing was performed at 400, 500 and 600°C for time periods ranging from 1 to 16 s. At temperatures of 500°C and below very little or no As was incorporated, indicating that the AsH_3 does not chemisorb at these temperatures. At 600°C the As incorporation appears to saturate at a at about $8x10^{13}$ cm^{-2} at exposure times above 8 s at a AsH_3 flow of 0.2 sccm. Similar results are expected for PH_3 growth.

We have also conducted experiments on p-type dopants using B_2H_6 - a gas source in an otherwise solid source MBE system. i.e., Si growth was by e-beam evaporation. At higher substrate temperatures (>550°C), B incorporation was linear with B_2H_6 exposure with an incorporation rate of about $(2\pm1)10^{-3}$ and at 550°C thus did not saturate even at a few Langmuirs of B_2H_6 exposure. At lower temperatures, we observe only a partial activation of the B (≤ 0.2), suggesting that the boron is still bound to hydrogen or does not occupy substitutional sites.

The experiments using APCVD for the controlled deposition of boron spikes into the Si layer were performed using a similar growth sequence as described for the As experiments. At temperatures ranging from 400 to 600°C well resolved boron spikes were observed, but no self limiting process has yet been found.

We are in the process of investigating these and similar ALE-type processes for dose control in both Si epitaxy and controlled diffusion sources in CMOS and bipolar technology.

4. Growth of III-Vs on Si and Ge

Building on previous experience with As, Sb and Ga stabilized growth of Ge on Si, and Si on Ge, we have extended our studies to investigate the role of Ga and As in the growth of Si and Ge on GaAs(001). These studies consist of two parts: (1) structure and

composition determination of clean, MBE grown GaAs(001) surfaces and (2) growth of Ge and Si on the GaAs(001)-c(2x8) surface.

(1) Structure and composition of clean GaAs(001)

In our previous Progress Report we described the development of a new high resolution Li^+ ion scattering technique. With this technique we obtain elemental resolution between Ga and As, and even between Ga, Ge and As, neighbours in the periodic system. Such high elemental resolution has not been reported previously. We have used this high resolution to study the structure and composition of the following clean GaAs(001) surfaces, from As-rich to Ga-rich: c(4x4), c(2x8), (2x4), c(8x2) and (2x6). For each surface the As/Ga ratio in the outer surface layers was determined quantitatively, and compared with generally accepted atomic models. It was found that in ALL cases, the surfaces are more Ga rich than previously believed. Atomic planes thought to be made up of As atoms alone are found to contain as much as 50 percent Ga! How this strong atomic-layer-mixing in the surface region will affect the epitaxial growth process in MBE,CVD and ALE conditions will be the subject of further studies.

(2) The As-rich c(2x8) surface was used as a starting surface for growth of thin Ge and Si layers. Excellent Ge layers can be grown both without and with an additional As flux. The presence of an excess As flux reduces, but does not eliminate the segregation of Ga to the Ge surface. The As sticking coefficient reduces to 0 when full monolayer coverage of As + Ga has been reached. Growth in the presence of an excess Ga flux is quite poor, leading to Ge islanding. Interdiffusion of Ge and GaAs (both during growth of Ge on GaAs and of GaAs on Ge) is a well known problem, leading to unintentional doping. Therefore we have attempted to use very thin Si films (less then 10 monolayers thickness) as a diffusion barrier between GaAs and Ge. While flat Si films could be grown successfully, we find that the crystal quality of the Ge film grown on top of the Si is poor, as determined from the channeling minimum yield. This result is rather surprising, since the Si thickness was kept well below the critical thickness. Even for a single monolayer of Si between GaAs and Ge, the Ge crystal quality appears to be negatively affected. In future studies we will attempt to grow a Ge/Si/Ge multilayer diffusion barrier, which could reduce the Ge source available to intermixing to less than a few times 10^{15} per cm^2.

Appendix A

J. Appl. Phys.,
submitted

GROWTH OF Si ON Si(100) VIA H/Cl EXCHANGE, AND THE EFFECT OF INTERFACIAL BORON

D. D. Koleske, S. M. Gates and D. B. Beach
IBM T. J. Watson Research Center, Yorktown Hts., NY 10598

ABSTRACT

Using alternating exposures of Si_2H_6 and Si_2Cl_6, very thin Si layers have been grown on the Si(100) surface at temperatures (T) as low as 475°C. Although this growth method is not truly self-limiting, some of the desired features for Si atomic layer epitaxy (ALE) are retained, as discussed here. The growth rate of new Si on Si(100) using this method is limited by the thermal desorption of H_2 and HCl. Doping the surface with boron atoms can lower the growth temperature, due to a weakening of the Si-H and Si-Cl bonds on the surface as observed in the temperature programmed desorption results from H_2, HCl and $SiCl_2$ desorption from the clean and the boron-doped Si(100) surfaces.

1. Introduction

The growth of II-VI and III-V semiconductor films in a self-limiting, layer-by-layer process using cycles of alternating exposure to two precursor gases is called Atomic Layer Epitaxy (ALE) {1,2}. Fine control over deposited film thickness with a uniform growth rate over large areas is characterisitic of this method. Both the growth rate (GR) per cycle and the spatial homogeneity are insensitive to small changes in process parameters. Recently, film growth {3,4} and surface chemistry {5-7} studies have considered the ALE deposition of Si from chlorosilanes. Each adsorption step is self-limiting because the surface dangling bonds (db) become terminated with either hydrogen or halogen atoms (Cl, for example), and db are required for adsorption of the precursor.

The "ideal" Si ALE process would be self-limiting, and would deposit one full monolayer (ML) of Si per cycle. In the case of binary II-VI or III-V semiconductors, one factor responsible for self-limiting adsorption is a difference in electronegativities between successive atomic layers and the partially ionic (polar) bonding between layers of *different electronegativities*. This aspect for self-limiting adsorption does not apply for elemental group IV semiconductors. In the group IV case, the bonding is highly covalent and adsorption is only limited by the number of surface db. One strategy for group IV ALE growth via successive deposition of identical layers is to alternately terminate the surface with atoms of different electronegativity, such as H and Cl, using appropriate Si precursors. Hypothetically, if the Si growth surface is fully terminated with either H or Cl and held at a low temperature (T), a reaction pathway based on an exothermic reaction (specifically HCl formation) might allow Si deposition to occur. Exothermic product (HCl) formation could provide some energy for local lattice annealing, producing Si epitaxy at low T, but this is only a speculation.

Here, we characterize a Si growth process consisting of alternating exposures of the Si(100) surface to Si_2Cl_6 and Si_2H_6. This process is not truly self-limiting, but retains some of the features described above. We use *in situ* time-of-flight (TOF) Scattering and Recoiling Spectroscopy (TOF-SARS), an analysis method recently reviewed by Rabalais {8,9}, to investigate the conditions for H/Cl exchange on Si(100) as a function of T. The TOF detection of recoiled atoms originating in the surface and formed by 2-body collision with energetic ions is known as direct recoiling (DR). A pulsed primary ion beam is used, which is 4 keV potassium (K^+) in this work. The TOF spectrum suffers from poor mass resolution, but DR is an excellent probe of surface hydrogen, and the degree of sensitivity to the 1st and deeper surface layers can be adjusted by changing the angle of incidence, α.

Starting with a Cl saturated Si(100) surface, we have measured the Si_2H_6 exposure required to completely exchange the Cl to H in the T range 450 - 550°C. This H-terminated surface is then dosed with Si_2Cl_6, exchanging the H-terminated surface to a Cl saturated surface. As the precursor gases adsorb onto the Si(100) surface at low T they deposit a submonolayer coverage of new Si, designated as Si^*. Deposition of Si^* from Si_2Cl_6 is self-limiting because all dangling bonds become saturated with Cl and this surface is stable at $T < 550°C$. Dosing with Si_2H_6 is used to remove the Cl as HCl, but deposition of Si^* from Si_2H_6 can occur via HCl or H_2 desorption, and this step is not self-limiting with respect to Si^* growth. The degree of order (epitaxial quality) of the Si^* layers grown here is unknown. In the future, we plan to study this important issue using electron diffraction. The T dependance of these exchange reactions is investigated over a narrow T range, and an interesting effect of boron on these reactions is then examined. Boron atoms distributed in the outermost surface layers are found to increase the rate of Cl → H exchange using Si_2H_6. Temperature programmed desorption (TPD) studies show a shift to lower T of the HCl desorption peak, and a shift in the threshold desorption T of $SiCl_2$ desorption. Thus, both TPD and exchange experiments indicate that boron weakens the adsorbed Cl to Si

bond, both with boron atoms in substitutional sites in the outer 1-3 surface layers, and with BH_x groups atop the 1st Si layer.

II. Experimental Details

The stainless steel UHV chamber has a base pressure of $3x10^{-10}$ torr, with partial pressures of gases other than H_2 and HCl less than $3x10^{-11}$ torr. A pulsed beam of 4 keV potassium ions (K^+) is incident on a Si(100) sample, with an available range of angle of incidence, α, of 0-30°. The angle between the incoming K^+ beam and the surface plane is defined as α, as shown previously {10}. The K^+ pulse width is $\simeq 10^{-8}$ s, and the beam current is $3x10^{-11}$ A (or less) in a rectangular spot of $\simeq 0.1$ cm^2 area. Elastic collisions at the surface form DR atoms (predominantly neutral), which have kinetic energies of a few hundred eV for H and $\simeq$ 2.3-2.4 keV for Si and Cl. These DR atoms are created from an impulsive 2-body collision {11}, and must have a direct line of site to both the K^+ beam and the detector.

The DR atoms are detected by exciting a microchannel plate at 39° recoil angle (Φ) after a flight path of 0.98 m. For any adsorbed element on the surface, we use changes in the DR peak height to give approximate changes in the relative coverage of that element. The DR peak heights are measured with respect to a flat baseline defined by extrapolation of the data at time-of-flight $< \simeq 4$ μs. A grid located in front of the detector is biased positively to reject scattered K^+ ions as shown elsewhere {12}, permitting detection of the chlorine (Cl_{DR}) DR peak, which would otherwise be obscured by the scattered K^+ peak. Effects of the primary K^+ beam have been examined and found undetectable when doses of 10^{-3}-10^{-2} ML of K^+ were used {12}. For all spectra shown here, the K^+ dose per spectrum is $< 10^{-3}$ ML (240 s, $3x10^{-11}$ A, area $\simeq 0.1$ cm^2). A series of 4-5 measurements results in $\simeq 0.005$ ML of K^+ ion dose. The K^+ beam is off except during signal averaging.

Temperature programmed desorption (TPD) experiments were performed in a separate UHV chamber with a sample to mass spectrometer distance of $\simeq$ 2 cm, using methods described previously {13}. Each TPD experiment monitored a single mass, with the mass spectrometer signal plotted directly on an XY recorder. The amplified thermocouple output was used to drive the X axis, to enhance the accuracy of the reported temperatures. The reactants Si_2H_6 and Si_2Cl_6 were introduced through a quartz dosing tube ending 2 cm. from the sample, with the flux adjusted with a leak valve. The Si_2H_6 was purchased from Matheson and was used without purification. The only detectable impurities were H_2 and SiH_4. The Si_2Cl_6 was purchased from Cambridge Isotopes and was purifed by fractional distillation on a 50 cm. column (packed with glass) under N_2 at P = 1 atm. The middle 3rd of the constant boiling fraction (145°C) was retained, and then degassed by 3 freeze, pump, thaw cycles. Boron was dosed as decaborane ($B_{10}H_{14}$), using a leak valve and a stainless steel collimating tube. All gas doses were measured approximately by reading the ion gauge pressure in the chamber without correction. The Si(100) surface was cleaned by Ar^+ sputtering at room T, annealing for 1-2 minutes at 900°C, slow cooling to 700°C and finally growing a fresh Si layer ($\simeq 10^3$ Å) from Si_2H_6 at 700°C.

III. Results and Interpretation

A. H / Cl Exchange Using Si_2H_6 and Si_2Cl_6

Initially, direct recoiling (DR) experiments were conducted using a fixed angle of incidence (α) of 3° with respect to the surface plane for the K^+ beam, to enhance sensitivity to the surface layers. (The effect of changing α on surface sensitivity will be discussed in Section III.D.) Figure 1 shows the DR results of a typical exchange experiment on Si(100) at a surface temperature (T) of 475°C. In Figure 1A, one peak from DR Si atoms (Si_{DR}) from the clean Si(100) surface is seen at 7.80 μs. The flat baseline in the vicinity of 5-6 μs is indicative of a clean surface. The surface was then exposed to 10^{19} Si_2Cl_6 cm^{-2} at 475°C, quenched to 200-300°C, and the resulting spectrum 1B was measured. In all cases, the surface was quenched immediately after exposure to the gases so that no desorption of

Cl or H occurred during data acquisition. Based on the work of Yarmoff and co-workers on Si(111) {14} and our own studies in which the Si_2Cl_6 exposure was varied, this spectrum should correspond to $\simeq$1 ML of monochloride species terminating all of the Si(100) dangling bonds. Only 10^{17} Si_2Cl_6 cm^{-2} is required to saturate the Cl_{DR} peak intensity. This surface is thermally stable at 475°C for times in excess of 30 minutes because at this T $SiCl_2$ desorption is slow. Exposing the monochloride surface to Si_2H_6 at 475°C, followed by quenching to lower T for data acquisition results in the spectrum shown in 1C. At this temperature complete removal of the surface Cl, and formation of a fully saturated monohydride surface is accomplished when 2 x 10^{20} Si_2H_6 cm^{-2} exposure is used. This experiment used a flux of $2x10^{17}$ Si_2H_6 $cm^{-2}s^{-1}$ x 1,000 s. Lower exposures result in partial Cl removal (data not shown). The Cl is removed from the surface via formation of HCl, as will be shown below using TPD. Finally, the monohydride surface is completely converted back to the monochloride terminated surface by exposing the surface to 10^{19} Si_2Cl_6 cm^{-2} at 475°C. The result is shown as spectrum 1D.

The exchange of H to Cl ($Si_2Cl_6 \rightarrow H$) is expected to be facile at 475°C, because H_2 desorption will occur on the timescale of 5-10 minutes at this temperature. This was observed by heating a H terminated surface up to 475°C. and recording the hydrogen DR (H_{DR}) signal as a function of time (data not shown). The H_{DR} signal decreased by approximately 5% per minute and the surface was clean after 15 minutes. The exchange of Cl to H ($Si_2H_6 \rightarrow Cl$) step is less rapid because the Cl must desorb as HCl, which is slower than H_2 desorption. The desorption of Cl as $SiCl_2$ is even slower than HCl desorption, and occurs only at higher T.

Experiments similar to that shown in Figure 1 were conducted as a function of T, with a summary shown in the top panel of Figure 2. The exposures required to give complete exchange of the surface H or Cl are plotted versus T. The $Si_2H_6 \rightarrow Cl$ reaction requires large exposures of Si_2H_6, with the exposure at each T indicated with triangles. The

$Si_2Cl_6 \rightarrow H$ reaction is more facile, and the Si_2Cl_6 exposure is indicated using squares. Above 500°C, H desorption from the surface becomes fast enough that very little Si_2Cl_6 is needed for complete H removal. At T ~ 500°C, larger doses of Si_2Cl_6 are needed to remove adsorbed H. Consistently, 10-100 times more Si_2H_6 is needed to remove adsorbed Cl than is needed for the removal of H.

The trend of decreasing exposure to give complete exchange as T is increased suggests that both exchange reactions are thermally activated, and we explore this conclusion using measured values of desorption kinetic parameters from the literature. The bottom panel of Figure 2 shows 1st order and pseudo-1st order desorption rates plotted versus surface T. The dashed line indicates the 1st-order desorption rate of H_2 from Si(100) plotted versus surface T, as reported by Sinniah and co-workers {15} with the pre-exponential $\nu = 2 \times 10^{11}$ s^{-1} and the desorption activation energy $E_D = 45$ Kcal/mole. Curves for desorption of HCl (solid line) and $SiCl_2$ (dot-dash line) from Si(111)-(7X7) using the data of Coon, George and co-workers {7} are also shown. Second order desorption is observed for both HCl and $SiCl_2$, with $\nu = 2500$ cm^2/s and $E_D = 72$ kcal/mole reported for HCl and $\nu = 3.2$ cm^2/s and $E_D = 67$ kcal/mole reported for $SiCl_2$ {7}. A single *assumed* coverage of 1/2 ML (3.4×10^{14} cm^{-2}) was used to compute pseudo-1st order rates for HCl and $SiCl_2$ desorption so that a grossly simplified, order of magnitude, comparison with H_2 is possible. The solid curve thus estimates a hypothetical HCl desorption rate vs. T for a constant coverage of 1/2 ML of H and 1/2 ML of Cl together on the Si(100) surface. The dot-dash curve estimates the hypothetical $SiCl_2$ desorption rate vs. T from 1/2 ML of Cl. Kinetics from Si(111) are used because no such data have been published for Si(100). The comparison in Figure 2 is considered further under Discussion.

B. Effects Of Boron On $Si_2H_6 \rightarrow Cl$ Reaction

In this section we show the effect of surface boron (B) on the $Si_2H_6 \rightarrow Cl$ exchange reaction. On the Si(100)-(2X1) surface, B atoms can be substitutionally incorporated into the outer 2 surface layers when evaporated B atoms are used {16} and with sufficiently low B coverage ($\simeq$ 1/2 ML), the surface remains well ordered after annealing at 700°C {17}. We now examine the behavior of B after $B_{10}H_{14}$ dosing and annealing. Figure 3 shows DR spectra with $\alpha = 3^o$ as a function of annealing T following $B_{10}H_{14}$ exposure. At 300°C the clean surface was dosed with $2x10^{16}$ $B_{10}H_{14}$ cm^{-2} and the DR signal measured (bottom panel). As the surface is heated the H_{DR} signal decreases accompanied by a decrease in the B_{DR} signal and an increase in the Si_{DR} signal. By $\simeq$ 600°C most of the H has desorbed from the surface and the B_{DR} signal reaches a value that remains constant up to $\simeq$ 750°C. Above this temperature the B_{DR} signal begins to decrease rapidly and is nearly gone at 850°C. We will address the depth distribution of B atoms later in section III.D.

To see if the B is desorbing or diffusing into the Si lattice, a TPD experiment was performed using the same $B_{10}H_{14}$ exposure (data not shown). During heating, H_2 desorption is first detected at $\simeq$ 300°C, and is abundant over the T range 400-650°C. The TPD signal from BH^+ was on the order of 1% of the H_2^+ signal. We assume that BH^+ would be a measurable cracking fragment of any and all B_xH_y species that might desorb. The amount of desorbing B is very small, yet the B_{DR} signal decreases dramatically. These results indicate that as hydrogen is evolved from the surface during annealing, most of the B migrates from the surface to occupy subsurface sites. This is complete at $\simeq$ 650°C. At T > 750°C boron rapidly diffuses into the bulk.

To demonstrate that new Si^* is grown on the surface using the $Si_2H_6 \rightarrow Cl$ and $Si_2Cl_6 \rightarrow H$ reactions, the surface was doped with B to provide an "elemental marker" layer.

The B_{DR} signal from this layer is attenuated as additional Si^* is grown above it {18}. The results in Figure 4 are similar to the spectra shown in Figure 1, except that the surface is initially doped with B, and the surface T = 400°C during the exchange reactions. The initially clean Si(100) surface was dosed with $2x10^{16}$ $B_{10}H_{14}$ cm^{-2} at 300°C, heated to 650°C, and spectrum 4A shows the resulting B_{DR} signal. Next this surface was heated to 400°C and dosed with $4x10^{19}$ Si_2H_6 cm^{-2}. The resulting spectrum is shown in Figure 4B after quenching the surface to 200-300 °C. This surface was then dosed with $2x10^{19}$ Si_2Cl_6 cm^{-2} at 400°C, quenched, and spectrum 4C was recorded. Next, this surface was dosed with $1x10^{20}$ Si_2H_6 cm^{-2} at 400°C., quenched, and spectrum 4D was measured. Finally, this surface was dosed with $5x10^{19}$ Si_2Cl_6 cm^{-2} at 400°C., quenched, and spectrum 4E was recorded. Notice that not all the surface H is removed and that exchange to a Cl-terminated surface is incomplete. The B layer is becoming "buried" by the growth of Si^*, and the B is no longer active in promoting H/Cl exchange at the surface.

Evidence that Si is in fact being grown on top of the initial B/Si(100) surface is seen in Figure 4 where the B_{DR} signal in 4C is roughly 1/2 the original B_{DR} signal in 4A. The H_{DR} peak in 4D renders the B marker not useful quantitatively in this case. In spectrum 4E, the B_{DR} peak is slightly smaller than in 4C. Although the surface chemistry is somewhat modified by the boron "marker" layer, it is evident from these spectra that new Si^* has been grown on top of the B/Si(100) surface.

Instead of annealing the surface up to 650°C after dosing with $B_{10}H_{14}$ (to remove H and place B atoms in the subsurface region), exchange experiments using a $B_{10}H_{14}$ saturated Si(100) surface at 400°C were performed. These results are shown in Figure 5. A clean Si(100) surface (spectrum 5A) was dosed with $2x10^{16}$ $B_{10}H_{14}$ cm^{-2} at 300°C (spectrum 5B). The surface in 5B is designated BH_x/Si(100). This surface was then heated to 400°C, which causes only a small change in the H coverage and no change in the DR signal from B or Si (see Figure 3). The surface in 5B was then dosed with $2x10^{19}$ Si_2Cl_6 cm^{-2}

at 400°C, and spectrum 5C was recorded. This exposure to Si_2Cl_6 at 400°C causes both the coverages of H and B to decrease to roughly 1/2 the initial values, and Cl is added to the surface. Next, the surface in 5C was dosed with $1x10^{20}$ Si_2H_6 at 400°C, and spectrum 5D was recorded. Finally, the surface in 5D was dosed with $3x10^{19}$ Si_2Cl_6 at 400°C, and spectrum 5E was measured. The reaction of Si_2Cl_6 with the BH_x terminated surface saturates at this point, as dosing with 3 times more Si_2Cl_6 did not remove any more H from the surface (data not shown).

Certain differences and similarities are seen for the surface covered with BH_x groups (Figure 5) compared to the surface having substitutional B atoms (Figure 4). The surface in Figure 5B should be fully covered with BH_x species. In the case of BH_x coverage, the H is not completely removed by Si_2Cl_6 exposure as seen in spectrum 5C. At 400°C, the $Si_2Cl_6 \rightarrow BH_x/Si(100)$ reaction does not go to completion. The B_{DR} signal in 5C is still relatively large. It is seen in Figures 4 and 5 that *Cl removal by Si_2H_6 is quite efficient at 400°C regardless of whether boron is present as atoms or as BH_x groups.* The B/Si(100) and BH_x/Si(100) surfaces appear similar in that spectra 4E and 5E are nearly identical. At 400°C, the B effects on the 2 exchange reactions are lost after a thin layer of Si^* is grown above the B layer. This is seen in the loss of complete exchange from 4D to 4E and from 5D to 5E. The location of the B layer at the end of this growth sequence can be studied further by changing the angle of incidence used in DR analysis, as shown below in Figures 7 and 8.

C. Effects Of Boron : TPD Studies

To further examine the effects of boron doping on the H and Cl exchange reactions and on the saturation coverages of H and Cl, TPD experiments were used. Figure 6 shows the TPD signals for H_2, HCl and $SiCl_2$ desorption from both the clean and B/Si(100) surfaces. Adsorption of Si_2H_6 (5 x 10^{19} cm^{-2} exposure) was used for the H_2 experiments, and

Si_2Cl_6 (5 x 10^{19} cm^{-2} exposure) was used for the $SiCl_2$ experiments. The HCl experiments used Si_2Cl_6 (5 x 10^{19} cm^{-2} exposure) followed by 5 x 10^{20} Si_2H_6 cm^{-2} exposure at 475 °C for the clean surface and at 400°C for B/Si(100). In Figure 6, two important effects are observed in the TPD profiles from clean Si(100) and B/Si(100) surfaces. First, the leading desorption edges of all three species are shifted to lower temperatures on the B/Si(100) surface relative to the clean Si(100) surface. The vertical arrows indicate the lowest T at which desorption is observed (desorption "threshold"). This implies a *weakening of both the Si-H and Si-Cl bonds at the surface when B is present.* Second, for H_2 and $SiCl_2$ the integrated peak area on the B/Si(100) surface is about 1/2 that on the clean surface. Since adsorption on the Si(100) surface occurs via chemisorption to the dangling bonds (db), this last result implies that the boron on the B/Si(100) surface has rendered 1/2 of the Si db inactive, or that B has replaced the Si atoms and completely removed 1/2 the db.

This coverage effect is also seen in the DR spectra. Comparison of DR spectra of the H saturated surfaces (after Si_2H_6 exposure) for the clean Si(100) surface (spectrum 1C) and the B/Si(100) surface (spectra 4B and 4D) confirms this effect. This can also be observed for the Cl saturated surface, although the poor mass resolution of DR prohibits quantitative comparison. Spectra 1B and 1D were measured on clean Si(100), while spectrum 4C was measured for the B/Si(100) surface.

D. DR Analysis Of B Location : Incident Angle, α, Scans

In order to examine the location of B atoms, and to monitor silicon growth on top of the boron doped layer, we measured the DR signal of various elements as a function of the incident angle, α. The DR atoms are formed by two body collisions between the incident K^+ and surface atom. Geometric lines of site from the collision point to the detector become significantly blocked for atoms in the third layer on the Si(100)-(2X1) surface at grazing incidence. At larger incident angles, geometric lines of site for the 3rd and 4th

layers open up. Therefore, the DR signal is sensitive to atoms in the 1st atomic layer at very low α, and signal from the 2nd and 3rd layers is *added to* the 1st layer signal as α is increased.

Spectra were collected for 120 s each at α value, and α was changed in 2-3° increments. The total K^+ beam damage accumulted in each α scan is less than 0.01 ML. At each value of α, the total DR signal is computed as the sum of the H, B, and Si peak heights. Again at each α, the fraction of the total signal that is contributed by one element is computed and this fraction is plotted versus α. We call such a plot an "α scan". By plotting the fraction of the total DR signal as a function of α, we can determine qualitatively whether each element is located at the surface or somewhat below the 1st layer. An α scan is shown in Figure 7 for the BH_x/Si(100) surface prepared by dosing with $2x10^{16}$ $B_{10}H_{14}$ cm^{-2} at a surface temperature of 200°C. At this low T, the B and H atoms lie above the outermost Si layer, although we do not know the stoichiometry or bonding site details of the BH_x fragments. In Figure 7, the H and B DR signals are large at small α. As α increases the H and B DR signals decrease and the Si DR signal increases. Signal originating from the surface layer decreases, and signal from deeper layers increases. In data which are not shown, when the BH_x/Si(100) surface is annealed up to 700°C (see Figure 3), producing the B/Si(100) surface, the B_{DR} signal *increases* for increasing α. This is consistent with B atoms located *below* the 1st surface layer.

In Figure 8 an α scan is shown for a thin Si layer grown at 400°C on top of the BH_x/Si(100) surface. Alternate exposures of Si_2H_6 and Si_2Cl_6 were used, exactly as in Figure 5. Following the study shown in Figure 5, the surface was dosed again with Si_2Cl_6. This was done to remove as much H as possible, so the H_{DR} signal would not interfere with the B_{DR} signal. The Cl_{DR} signal (squares) decreases with increasing α because Cl is terminating the surface. (This trend is similar to B and H in Figure 7.) The Si_{DR} signal increases as α increases similar to the Si behavior in Figure 7. The B_{DR} signal is

weak, however the B_{DR} signal increases slightly as α is increased. This behavior of the B_{DR} signal clearly shows the B layer is *not* at the surface. We conclude that new Si^* has been grown on top of the BH_x surface, using the Si_2H_6 and Si_2Cl_6 alternate exposures.

IV. Discussion

We have investigated the reaction of Si_2H_6 with a fully Cl-terminated Si(100) surface ($\Theta_{Cl} \simeq 1$), which we abbreviate $Si_2H_6 \rightarrow Cl$, and the reaction of Si_2Cl_6 with a fully H-terminated surface ($\Theta_H \simeq 1$), which we abbreviate $Si_2Cl_6 \rightarrow H$. Throughout the T range 450-550°C, the $Si_2Cl_6 \rightarrow H/Si(100)$ reaction proceeds 10-100 times faster than the $Si_2H_6 \rightarrow Cl/Si(100)$ reaction. Exposures on the order of 10^4 to 10^6 ML are required to complete the exchange reactions at 450°C. Attenuation of the DR signal from a boron "elemental marker" layer was used to demonstrate that new Si^* was in fact grown on top of the original Si(100) surface. We have recently observed similar attenuations in the Ge and Sn DR intensities when the Ge/Si(100) or Sn/Si(100) surfaces are dosed with Si precursor gases {18}.

We have interpreted the decrease in B_{DR} signal in terms of Si^* grown on top of the B marker. In TPD experiments that are not shown, we searched for desorption of BCl_3 and BH_xCl_{3-x} species following exposure of both the B/Si(100) and BH_x/Si(100) surfaces to Si_2Cl_6 at 400 °C. No desorption signals for such species could be observed, so we are confident that the effect we have called "attenuation" of the B_{DR} signal is *not* due to removal of B from these surface as BCl_3 or BH_xCl_{3-x}.

We consider the mechanisms of the 2 exchange reactions conducted at a typical T = 475°C. Pseudo-1st order desorption rates were shown plotted versus T in Fig. 2 for HCl and $SiCl_2$, using measured desorption kinetic parameters of Coon, George and co-workers {7} for HCl and $SiCl_2$ from Si(111)-(7X7). *Assumed fixed coverages* of H and Cl were used

in order to make a simple comparison with H_2 desorption. It is seen that HCl desorption is 10-100 times faster than $SiCl_2$ desorption at any given T, and in the mechanisms below we therefore write HCl desorption as the only path for Cl removal. At 475°C, the $SiCl_2$ pseudo-1st order desorption rate is $< 10^{-4}\ s^{-1}$, and the Cl-terminated surface is stable for over 1/2 hour at this T. During the conversion of a Cl-terminated surface to a H-terminated surface by Si_2H_6 exposure, both H_2 desorption and HCl desorption occur. Our largest Si_2H_6 exposures required on the order of 1,000 s, and the HCl pseudo-1st order desorption rate is $\simeq 10^{-3}\ s^{-1}$. During the $Si_2H_6 \rightarrow Cl$ reaction, new Si^* is deposited from Si_2H_6 via HCl desorption *and* there is also Si^* from Si_2H_6 growth via thermal H_2 desorption. This reaction is therefore not self-limiting concerning the growth of Si^*. The net reaction $Si_2H_6 \rightarrow Si^* + H_2$ *and* a reaction resulting in Cl removal as HCl both occur, so the total amount of Si^* deposited during this step is unknown, and will vary with details of the exposure (T, time, flux).

Two possible mechanisms for the reaction of Si_2H_6 with Cl-terminated Si(100) are considered here, and both assume a physisorbed, or molecular precursor, state of the Si_2H_6 molecule as the starting point {19, and references therein}. These are schematic mechanisms for discussion purposes, and are therefore not stoichiometric. The symbol __ is used to represent a dangling bond (db) on a surface Si atom. Mechanism A is initiated by the slow, infrequent desorption of $SiCl_2$.

$$\underline{Si}Cl + \underline{Cl} \rightarrow SiCl_2(g) + 2\ \_\_ \qquad (1)$$

$$Si_2H_6(p) + 6\ \_\_ \rightarrow 2\ \underline{Si}H + 4\ \underline{H} \qquad (2)$$

$$Si_2H_6(p) + 2\ \_\_ \rightarrow \underline{Si}H + \underline{H} + SiH_4(g) \qquad (3)$$

$$\underline{Cl} + \underline{H} \rightarrow HCl(g) + 2\ \_\_ \qquad (4)$$

$$2\ \underline{H} \rightarrow H_2(g) + 2\ \_\_ \qquad (5)$$

Notice that the initial step in this mechanism, reaction (1), involves removal of Si from the surface. Either reaction (2) or (3), or possibly both reactions, represent the adsorption of Si_2H_6 onto db, as discussed elsewhere {19}.

Mechanism B is initiated by the dissociation of Si_2H_6 in the precursor state to SiH_4 + SiH_2, and then insertion of the silylene diradical into an Si-Cl surface bond (reaction (7)).

$$Si_2H_6(p) \rightarrow :SiH_2(p) + SiH_4(g) \qquad (6)$$

$$:SiH_2(p) + \underline{Cl} \rightarrow \underline{Si}ClH_2 \qquad (7)$$

The species $\underline{Si}ClH_2$ could decompose directly to HCl(g) and $\underline{Si}H$, or could decompose on the surface followed by reaction (4) generating db for further reaction. Our data cannot address the distinction between mechanisms A and B. The $Si_2H_6 \rightarrow Cl$ step is not self-limiting because $\underline{Si}H$ species on the surface will undergo reaction (5) to $H_2(g)$ more rapidly than HCl desorption, reaction (4). This can be seen in Figure 2. The pseudo-1st order rate for desorption of H_2 is $\simeq$ 50 times the rate for desorption of HCl at 475°C.

The reaction $Si_2Cl_6 \rightarrow H$ is probably initiated by reaction (5) (thermal desorption of H_2), although this is a speculation. Reactions (8) and (9)+(10) describe 2 possible Si_2Cl_6 adsorption reactions.

$$Si_2Cl_6(p) + 6\ \_\_ \rightarrow 2\ \underline{Si}Cl + 4\ \underline{Cl} \qquad (8)$$

$$Si_2Cl_6(p) \rightarrow :SiCl_2(p) + SiCl_4(g) \qquad (9)$$

$$:SiCl_2(p) + \underline{H} \rightarrow \underline{Si}HCl_2 \qquad (10)$$

Removal of H from the surface is more likely by H_2 desorption than by HCl desorption as previously stated, however a significant amount of HCl is found in the TPD desorption profiles. This means that HCl formation might occur locally where Si_2Cl_6 reacts and de-

composes on the surface to SiCl. It has been shown that only monochloride species are stable on Si(111) above 300°C {14}, with dichloride and trichloride species being unstable. Upon completion of dosing with Si_2Cl_6, all Si "dangling" bonds are Cl terminated and $\Theta_{Cl} \simeq 1$. Desorption of $SiCl_2$ is slow at 475°C, so the $Si_2Cl_6 \rightarrow H$ reaction is self-limiting in that no additional Si_2Cl_6 can be adsorbed onto the Cl terminated surface (after all the H has been removed as HCl).

It appears that the general factor limiting the rate of both the $Si_2H_6 \rightarrow Cl$ or $Si_2Cl_6 \rightarrow H$ exchange reactions is the availability of dangling bonds for precursor gas adsorption. In schemes for Si ALE, one might consider using brominated or iodinated Si precursors. Recently, it has been shown that HBr desorbs near 510°C {20} and HI is believed to desorb at a temperature lower than 450°C. Having the product desorption channel (HBr or HI) active at a temperature lower than the desorption of either H_2 or SiX_2 might appear desirable. However, *it is specifically the slow rate of $SiCl_2$ desorption at a T where HCl desorption is sufficiently rapid* that makes the H + Cl system most suited for Si ALE.

We notice two major differences in the growth of Si^* on the B/Si(100) surface compared to growth of Si^* on the clean Si(100) surface. The first difference is that using cyclical doses of Si_2H_6 and Si_2Cl_6 the growth temperature can be lowered by 75-100°C on the B/Si(100) surface compared to clean Si(100). This implies that the subsurface boron is weakening the Si-Cl and Si-H bonds at the surface, causing HCl desorption to be more rapid, and allowing exchange reactions to occur at lower temperatures. This is verified in the lowering of the threshold desorption temperature of HCl and $SiCl_2$ in the TPD experiments shown in Figure 6.

A second effect of surface boron atoms was also observed. Both the TPD results and the DR spectra indicate that the saturation coverage of H or Cl on the B/Si(100) surface is $\simeq$ 1/2 the coverage compared to clean Si(100). A similar effect was reported for the

saturation coverage of atomic H on Si(111) following B doping {21}. In the H_2 TPD spectra in Figure 6, it is also seen that the ratio of β_2 to β_1 desorption features is larger on the B/Si(100) surface compared to the clean surface. Previously, it has been shown in low T adsorption studies using SiH_4 {13}, H_2O {22} and NH_3 {23} that the number of dangling bonds at the surface limits the adsorption of these molecules. Once the available db are saturated with adsorbates, the surface becomes relatively inert to further adsorption {13,22,23}. This suggests that on the B/Si(100) surface $\simeq$ 1/2 of the Si db have been eliminated by replacement with substitutional B, or have been rendered inactive by coordination to subsurface B. The latter effect has been observed on Si(111)-(7X7), where the B atoms are subsurface {24,25}. Feldman and co-workers have recently demonstrated that 1/2 ML of B atoms on Si(100) can be distributed in the 1st and 2nd Si layers {16}, and that epitaxial Si can be readily grown on this B layer by molecular beam epitaxy {17}, resulting in a δ-doped, B layer buried within the epitaxial Si. In our case, roughly 1/2 of the "dangling" bonds have been effectively removed from the B/Si(100) surface, and Si^* growth on B/Si(100) should be different than Si^* growth on clean Si(100). Specifically, the new Si^* grown on the B/Si(100) surface may contain a large number of defects near the Si^*/B/Si(100) interface if Si^* atoms do not readily occupy lattice sites above the inactive db. In future studies, we plan to use electron diffraction to examine the epitaxial quality of Si^* layers and B effects.

The literature provides some information on the addition of B to the Si(100) surface. Yu and co-workers {26} measured a downward shift in the Fermi level of Si(100) toward the valence band of 0.4 eV with $\simeq$ 1/3 ML of B atoms present. This effect saturated, with higher B coverage having no more effect. Also, it is well known that the Si lattice constant contracts upon addition of B {27}. On Si(111)-(7X7), subsurface B atoms withdraw electron density from the dangling bonds, rendering the surface somewhat inert {25,28}. Thus, our B/Si(100) surface is electron deficient and the lattice is probably slightly contracted, compared to clean Si(100)-(2X1).

Certain differences were observed in the growth of Si^* on top of the B/Si(100) annealed surface (Figure 4) compared to the surface containing a high coverage of BH_x groups (Figure 5). A major difference is that not all of the H on the BH_x/Si(100) surface can be removed using Si_2Cl_6 at 400°C. The reaction of Si_2Cl_6 with the BH_x/Si(100) surface stops at 400°C with roughly 1/2 the H removed. We noted that increasing the Si_2Cl_6 dose by 3 times caused no further reaction (Figure 5). The reason may be that some of the H is bonded to Si, and this is susceptible to reaction with Si_2Cl_6 The H that remains after Si_2Cl_6 reaction may be bonded to B. Using gas phase thermochemical bond energies, the B-H bond ($\simeq$ 90 Kcal/mole) is stronger than the Si-H bond ($\simeq$ 80 Kcal/mole) {29,30}. The $Si_2H_6 \rightarrow Cl$ reaction appears to proceed completely on this surface. Once the Si_2H_6 is dosed the B_{DR} signal drops significantly. It is seen in Figures 4 and 5 that *Cl removal by Si_2H_6 is quite efficient at 400°C regardless of whether boron is present as atoms or as BH_x groups*. Inspection of spectra 4E and 5E showed that these surfaces with a "buried" (attenuated) B layer give indistinguishable DR spectra.

Qualitative aspects of the location of adsorbed boron (residing on the surface or in the subsurface region) were addressed by monitoring the elemental DR signals as a function of incident angle, α. As shown in Figures 7 and 8, elements which are located on top of the surface have DR signals that decrease as α is increased, while elements with a large concentration in the subsurface region have an increase in the DR signal as α is increased. Although these signatures are quite conclusive from the data in Figures 7 and 8 regarding the general location of the B layer, the actual binding sites in the subsurface region can not be determined. Subsurface B could sit in any layer (second, third, etc.) and the simple α scans cannot distinguish between these different adsorption sites. Azimuth angle scans and simulations may be used to address the site(s) for B in the future. The α scan in Figure 8 does prove that a very thin Si^* layer is grown by alternate Si_2Cl_6 and Si_2H_6 reactions in the experiment shown in Figure 5 on the BH_x/Si(100) surface, because the B layer is behaving like a buried layer and not like an element in the 1st layer.

V. Summary

This study of H/Cl exchange on the Si(100) surface has the following implications for growth of thin Si layers by ALE.

1. The stable, commercially available molecules Si_2H_6 and Si_2Cl_6 form a viable pair of reactant molecules for Si growth using cycles of alternating gas exposures in the T range 450-500°C.
2. This scheme is not truly self-limiting but it does retain some of the desirable features of true ALE growth.
3. Simple thermal desorption of HCl and H_2 products explains the observed T dependance of this exchange chemistry. Formation of the H-Cl bond in the HCl product desorption step does not appear to "assist" the growth process by contributing any energy to the Si surface.
4. Doping the surface with BH_x groups or with B atoms lowers the T for H/Cl exchange, by weakening both the Si-Cl and Si-H surface bonds.

Acknowledgements

This work is supported by the Office of Naval Research under contract # N00014-91-C-0080. The authors thank Dr. J. A. Schultz for discussions of direct recoiling analysis.

REFERENCES

1. T. Suntola and M. Simpson (Eds.); "Atomic Layer Epitaxy", Chapman and Hall, NY, NY; copyright 1990 by Blackie & Son, Ltd., London.
2. C.H.L. Goodman and M.V. Pessa; J. Appl. Phys. **60** (1986) R65.
3. D. Lubben, R. Tsu, T.R. Bramblett and J.E. Greene, J. Vac. Sci. Tech. A **9**, 3003 (1991).

4. J. Nishizawa, K. Aoki, S. Suzuki and K. Kikuchi, J. Crystal Growth **99**, 502 (1990).

5. J.A. Yarmoff, D.K. Shuh, T.D. Durbin, C.W. Lo, D.A. Lapiano-Smith, F.R. McFeely and F.J. Himpsel; J. Vac. Sci. Tech., in press.

6. Y. Takahashi and T. Urisu; Jap. J. Appl. Phys. **30**, L209 (1991).

7. P.A. Coon, P. Gupta, M.L. Wise and S.M. George; J. Vac. Sci. Tech. A **10**, 324 (1992).

8. J.W. Rabalais; Science **250**, 522 (1990).

9. J.W. Rabalais, CRC Crit. Rev. Solid State Mater. Sci. **14**, 319 (1988).

10. S. M. Gates, C.-M. Chiang and D. B. Beach; J. Appl. Phys., in press.

11. S. Chaudhury and R. S. Williams; Surf. Sci. **255**, 127 (1991).

12. S.M. Gates and S.K.Kulkarni; Appl. Phys. Lett. **60**, 53 (1992).

13. S.M. Gates, C.M. Greenlief, and D.B. Beach; J. Chem. Phys. **93** , 7493 (1990)

14. L.J. Whitman, S.A. Joyce, J.A. Yarmoff, F.R. McFeely and L.J. Terminello; Surf. Sci. **232**, 297 (1990).

15. K. Sinniah, M. G. Sherman, L. B. Lewis, W. H. Weinberg, J. T. Yates, Jr. and K. C. Janda; J. Chem. Phys. **92**, 5700 (1990).

16. B.E. Weir, R.L. Headrick, Q. Shen, L.C. Feldman, T.R. Hart, M. Needels, M.S. Hybertson and M. Schluter; to be published.

17. R.L. Headrick, B.E. Weir, A.F.J. Levi, D.J. Eaglesham and L.C. Feldman; Appl. Phys. Lett. **57**, 2779 (1990).

18. S.M. Gates and D.D. Koleske; Appl. Phys. Lett., submitted.

19. S.M. Gates and C.-M. Chiang; Chem. Phys. Lett. **184**, 448 (1991), and references therein.

20. C.C. Cheng, S.R. Lucas, H. Gutleben, W.J. Choyke, and J.T. Yates, J. Am. Chem. Soc. **114**, 1249 (1992).

21. P.J. Chen, M.L. Colaianni and J. T. Yates; J. Appl. Phys. **70**, 2954 (1991).

22. B.G. Koehler, C.H. Mak and S.M. George; Surf. Sci. **221**, 565 (1989).

23. F. Bozso and Ph. Avouris; Phys. Rev. Lett. **57**, 1185 (1986).

24. I.W. Lyo, E. Kaxiras and Ph. Avouris; Phys. Rev. Lett. **63**, 1261 (1989).

25. Ph. Avouris, I.W. Lyo, F. Bozso and E. Kaxiras; J. Vac. Sci. Tech. **A8**, 3405 (1990).

26. M.L. Yu, D.J. Vitkavage and B.S. Meyerson J. Appl. Phys. **59**, 4032 (1986).

27. W.B. Pearson, "A Handbook of Lattice Spacings and Structures of Metals and Alloys", Pergamon Press, Oxford, (1967); F.H. Horn, Phys. Rev. **97**, 1521 (1955).

28. F. Bozso and Ph. Avouris; Phys. Rev. B. **44**, 9129 (1991).

29. R. Walsh, *Acc. Chem. Res.*, **14** (1981) 246.

30. W.L. Jolly, "Modern Inorganic Chemistry", McGraw-Hill, NY.

FIGURE CAPTIONS

FIGURE 1. TOF-DR spectra from Si(100)-(2X1) surface using a 4 keV K^+ beam, with an incident angle, α, of 3° with respect to the surface plane and a recoil angle, Φ, of 39°. Each spectrum is signal averaged for 240 seconds. This figure shows the Si_2H_6 and Si_2Cl_6 exchange reactions for a surface temperature of 475°C. A: TOF spectrum from a clean Si(100) surface where the Si_{DR} peak appears at 7.80 μs. B: Surface after dosing with Si_2Cl_6 and the Cl_{DR} peak appears at 8.66 μs. C: Surface after dosing with Si_2H_6 and the H_{DR} peak appears at 4.65 μs. D: Surface after another dose with Si_2Cl_6.

FIGURE 2. Top Panel: Exposures required to perform the $Si_2H_6 \rightarrow Cl$ reaction using Si_2H_6 (triangles), and the $Si_2Cl_6 \rightarrow H$ reaction using Si_2Cl_6, plotted vs. surface temperature. Bottom Panel: Pseudo-1st order desorption rates for HCl and $SiCl_2$ and true 1st order desorption rate for H_2 plotted as a function of temperature.

FIGURE 3. $B_{10}H_{14}$ decomposition on the Si(100) surface as a function of temperature using DR with $\alpha = 3°$. The bottom spectrum shows the surface DR spectrum after dosing with $B_{10}H_{14}$ at 300°. Each subsequent spectrum shows the signal after increasing the temperature. Notice that the decrease in the B_{DR} signal coincides with the decrease in the H_{DR} signal.

FIGURE 4. Si_2H_6 and Si_2Cl_6 exchange spectra measured for the boron doped Si(100) surface, similar to Figure 1. The B_{DR} peak appears at 5.79 μs. A: $B_{10}H_{14}$ dosed and annealed, giving the B/Si(100) surface. B: B/Si(100) surface dosed with 4 x 10^{19} Si_2H_6 cm^{-2}. C: Surface in B, dosed with 2 x 10^{19} Si_2Cl_6 cm^{-2}. D: Surface in C, dosed with 1 x 10^{20} Si_2H_6 cm^{-2}. E: Surface in D, dosed with 5 x 10^{19} Si_2Cl_6 cm^{-2}.

FIGURE 5. Si_2H_6 and Si_2Cl_6 exchange reactions on the $B_{10}H_{14}$ dosed, but not annealed Si(100) surface, designated BH_x/Si(100), similar to Figure 4. A: Clean Si(100) surface. B: Spectrum after dosing with 2 x 10^{16} $B_{10}H_{14}$ cm^{-2} at 300°C. C: Surface in B, dosed with 2 x 10^{19} Si_2Cl_6 cm^{-2}. D: Surface in C, dosed with 6 x 10^{19} Si_2H_6 cm^{-2}. E: Surface in D, dosed with 3 x 10^{19} Si_2Cl_6 cm^{-2}.

FIGURE 6. TPD spectra measured on the clean and B/Si(100) surfaces. From top to bottom, the top spectra are H_2 (2 amu) from the B doped and clean surfaces, each following a Si_2H_6 exposure of 5 x 10^{19} cm^{-2}. The middle spectra are HCl (36 amu) from the B doped and clean surfaces, each following an Si_2Cl_6 exposure of 5 x 10^{19} cm^{-2} and a Si_2H_6 exposure of 5 x 10^{20} cm^{-2} (at 475°C for clean Si(100), and at 400°C for B/Si(100)). The bottom spectra are $SiCl_2$ (63 amu) from the B doped and clean surfaces, each following an Si_2Cl_6 exposure of 5 x 10^{19} cm^{-2}. The heating rate was $\simeq$ 4°C/second.

FIGURE 7. Incident angle, α, scan for BH_x/Si(100). The fraction of the total DR signal contributed by each element is plotted as a function of α for H, B, and Si. The spectra were measured for 120 seconds each after dosing with $B_{10}H_{14}$ at 300° and quenching the surface temperature below 300°. Elements located on the surface show a decrease in signal as α is increased, while elements located below the 1st surface layer show an increase in signal as α is increased. This is discussed in detail in the text.

FIGURE 8. Incident angle, α, scan for the surface prepared in Figure 4, and with an additional dose of Si_2Cl_6 added. The fraction of the total DR signal contributed by each element is plotted as a function of α. Here the B_{DR} signal increases as α is increased, indicating that B is located beneath the surface and new Si^* has been grown on the BH_x/Si(100) surface.

Fig. 1

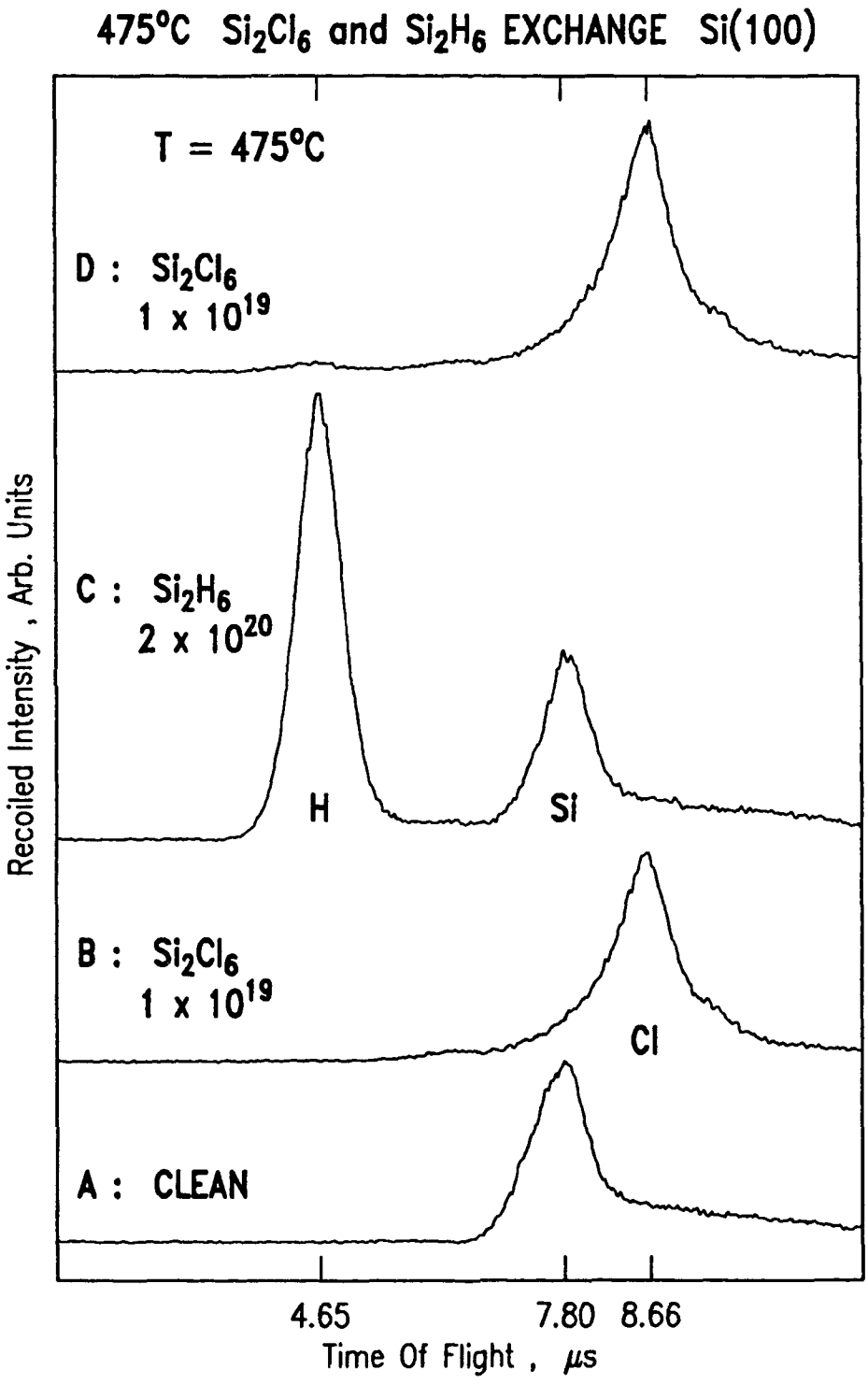
475°C Si_2Cl_6 and Si_2H_6 EXCHANGE Si(100)
T = 475°C
D : Si_2Cl_6
1 x 10^{19}
C : Si_2H_6
2 x 10^{20}
H
Si
B : Si_2Cl_6
1 x 10^{19}
Cl
A : CLEAN
Recoiled Intensity , Arb. Units
4.65
7.80
8.66
Time Of Flight , μs

Fig. 2

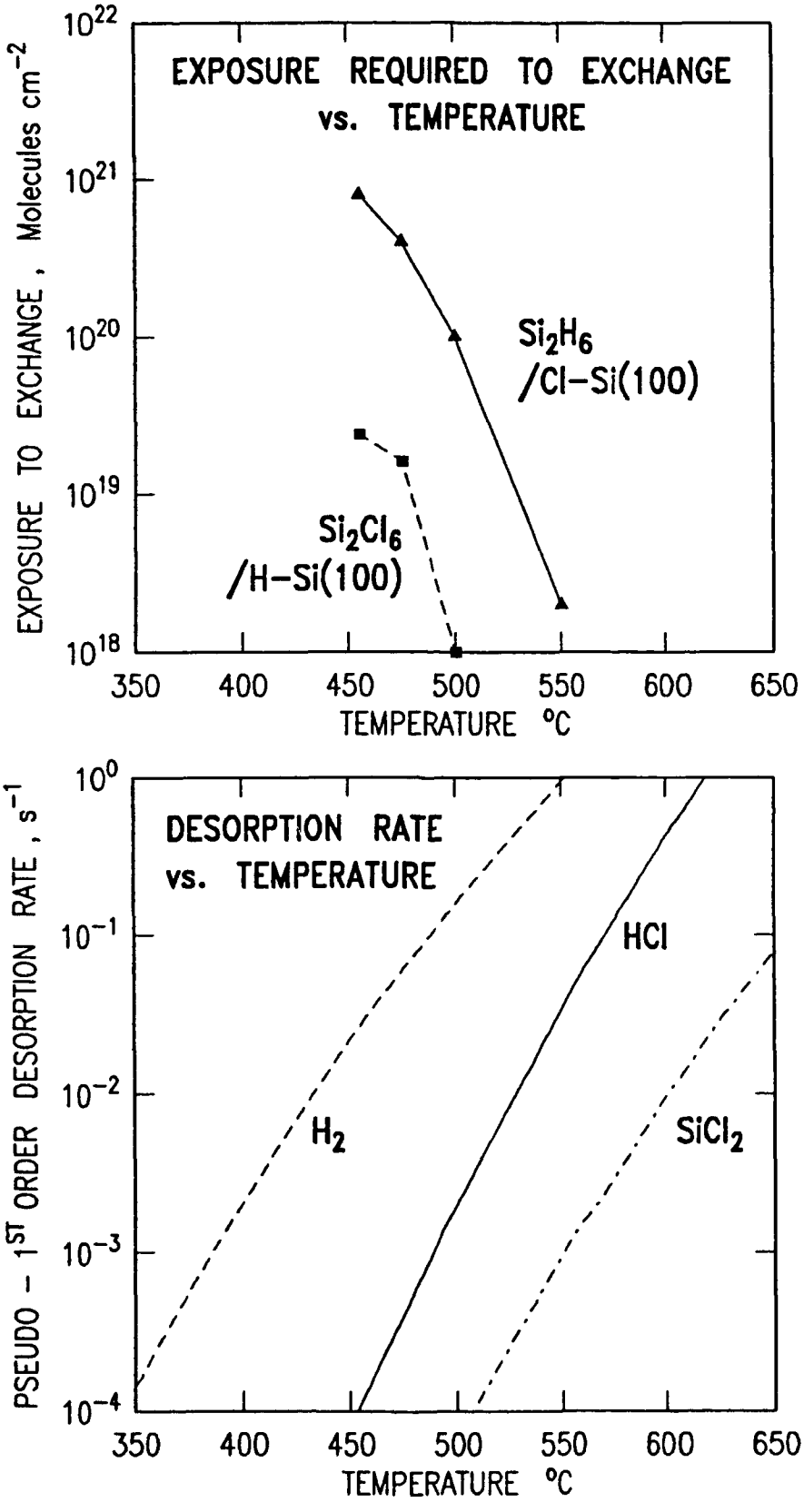
EXPOSURE REQUIRED TO EXCHANGE
vs. TEMPERATURE
EXPOSURE TO EXCHANGE, Molecules cm^{-2}
10^{22}
10^{21}
10^{20}
10^{19}
10^{18}
Si_2H_6
/Cl-Si(100)
Si_2Cl_6
/H-Si(100)
350
400
450
500
550
600
650
TEMPERATURE °C
DESORPTION RATE
vs. TEMPERATURE
PSEUDO - 1ST ORDER DESORPTION RATE, s^{-1}
10^{0}
10^{-1}
10^{-2}
10^{-3}
10^{-4}
HCl
H_2
$SiCl_2$
350
400
450
500
550
600
650
TEMPERATURE °C

Fig. 3

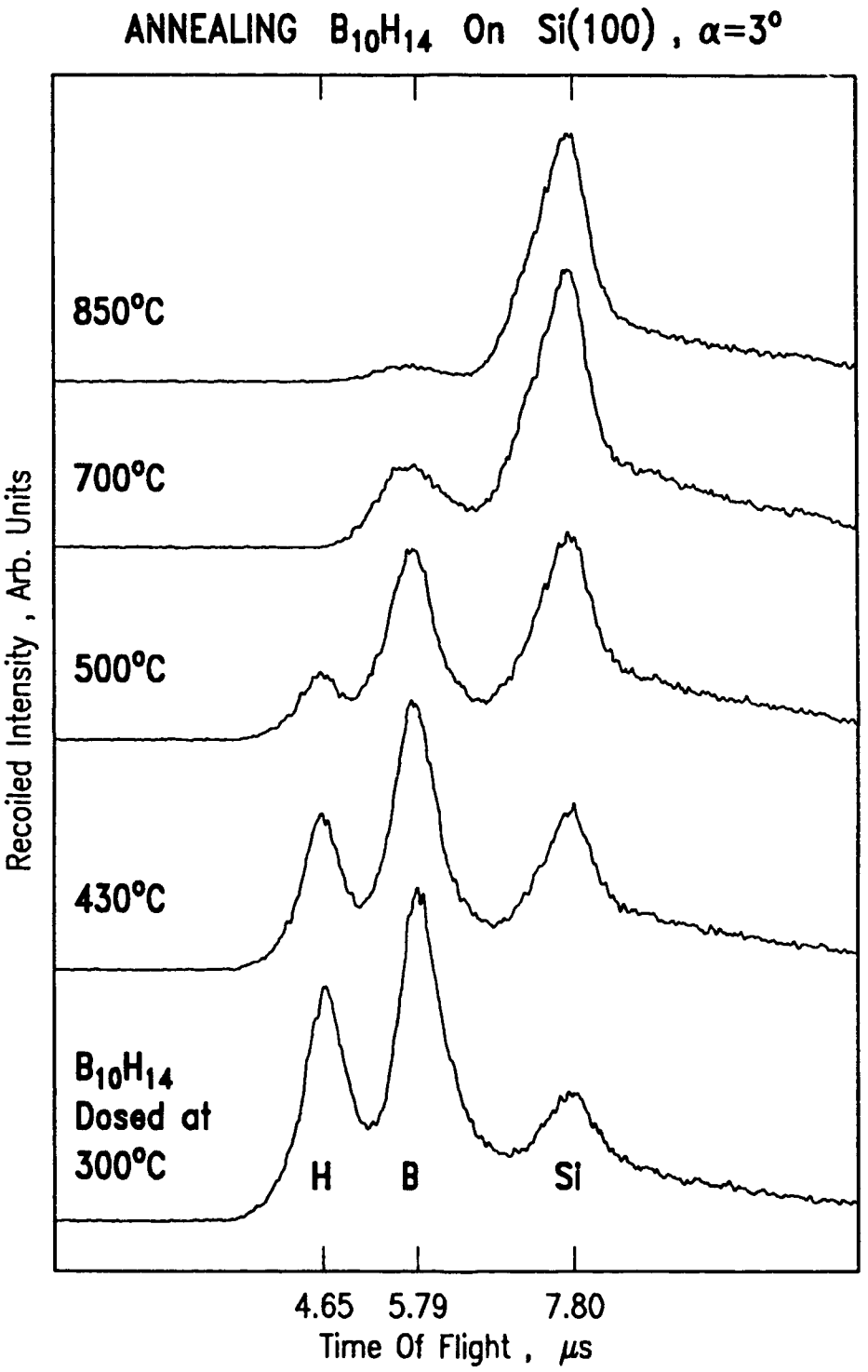
ANNEALING $B_{10}H_{14}$ On Si(100) , α=3°
850°C
700°C
500°C
430°C
$B_{10}H_{14}$ Dosed at 300°C
H
B
Si
Recoiled Intensity , Arb. Units
4.65
5.79
7.80
Time Of Flight , μs

Fig. 4

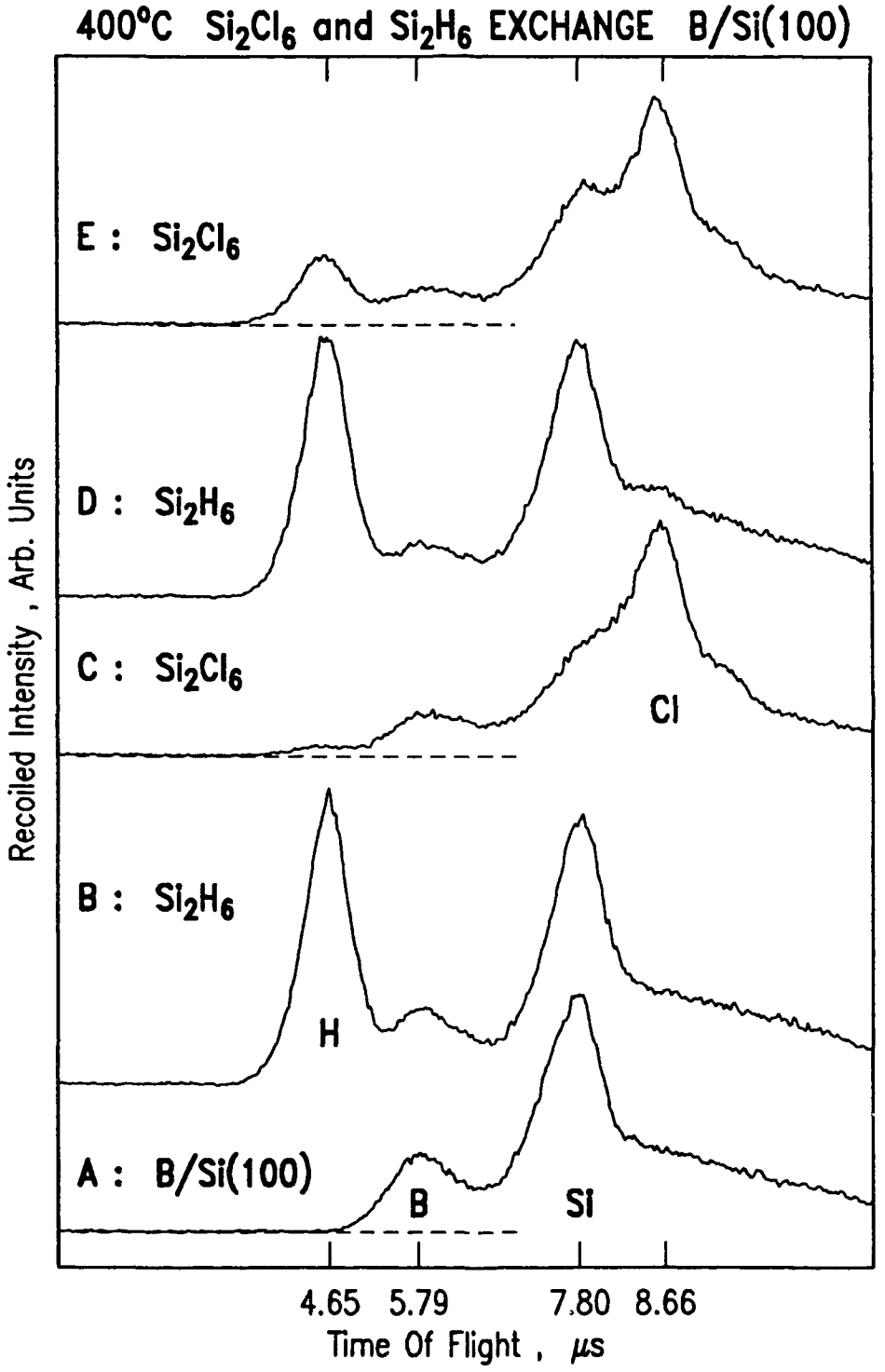
400°C Si_2Cl_6 and Si_2H_6 EXCHANGE B/Si(100)
E : Si_2Cl_6
D : Si_2H_6
C : Si_2Cl_6
Cl
B : Si_2H_6
H
A : B/Si(100)
B
Si
Recoiled Intensity , Arb. Units
4.65
5.79
7.80
8.66
Time Of Flight , μs

Fig. 3

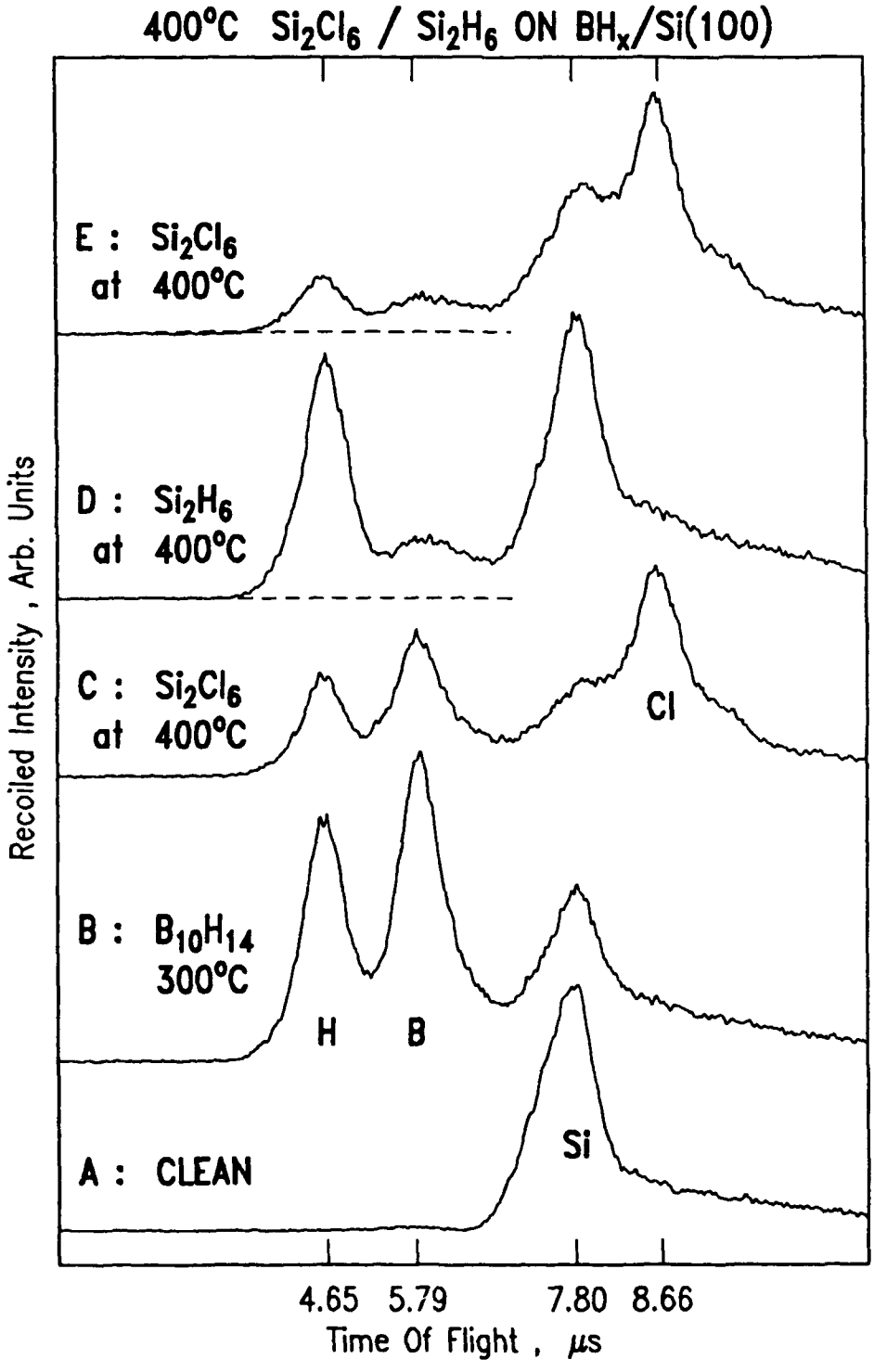
400°C Si2Cl6 / Si2H6 ON BHx/Si(100)
E : Si2Cl6 at 400°C
D : Si2H6 at 400°C
C : Si2Cl6 at 400°C
Cl
B : B10H14 300°C
H
B
A : CLEAN
Si
Recoiled Intensity , Arb. Units
4.65
5.79
7.80
8.66
Time Of Flight , μs

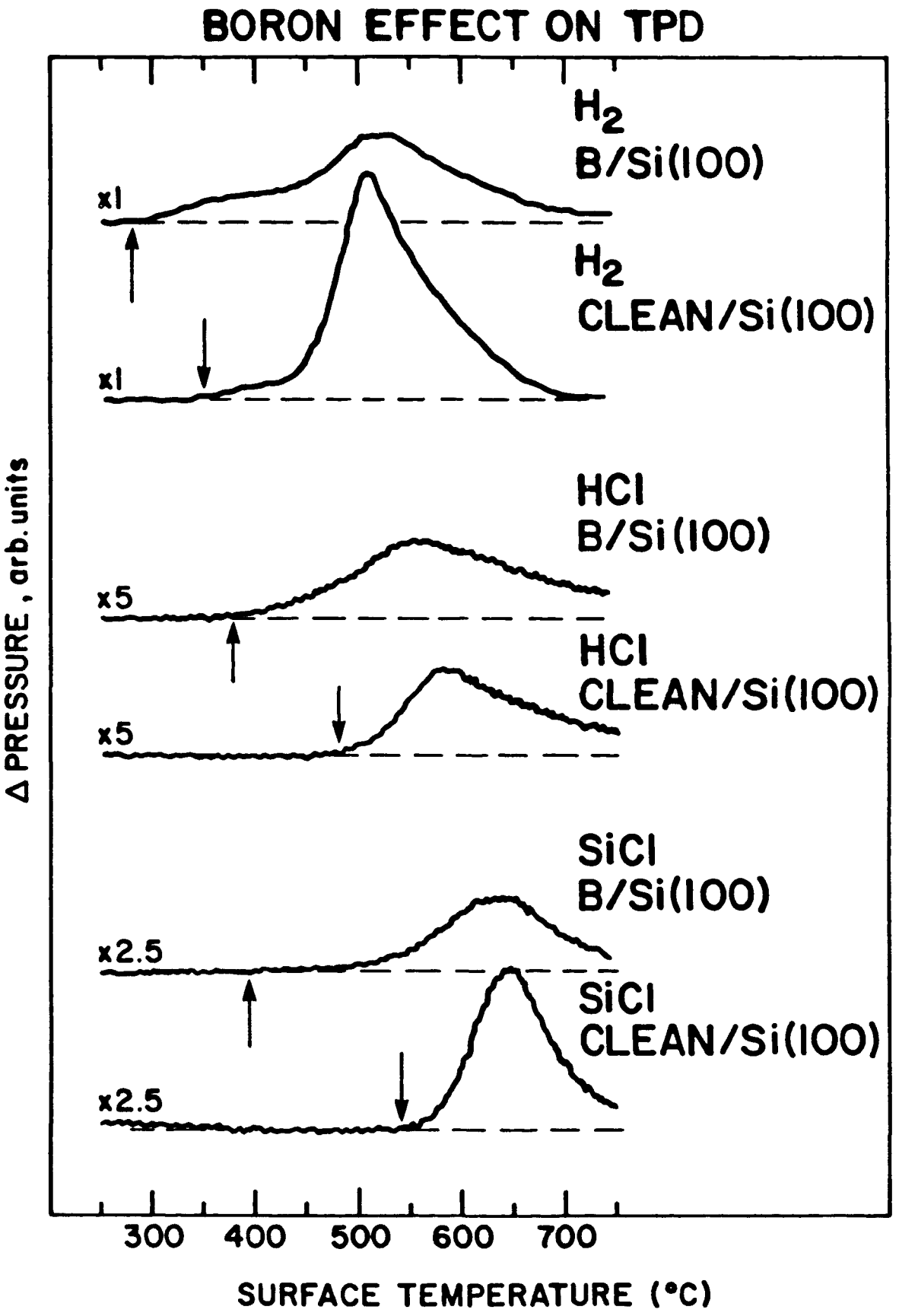
BORON EFFECT ON TPD
H2
B/Si(100)
x1
H2
CLEAN/Si(100)
x1
HCl
B/Si(100)
x5
HCl
CLEAN/Si(100)
x5
SiCl
B/Si(100)
x2.5
SiCl
CLEAN/Si(100)
x2.5
Δ PRESSURE, arb. units
300
400
500
600
700
SURFACE TEMPERATURE (°C)

Fig. 7

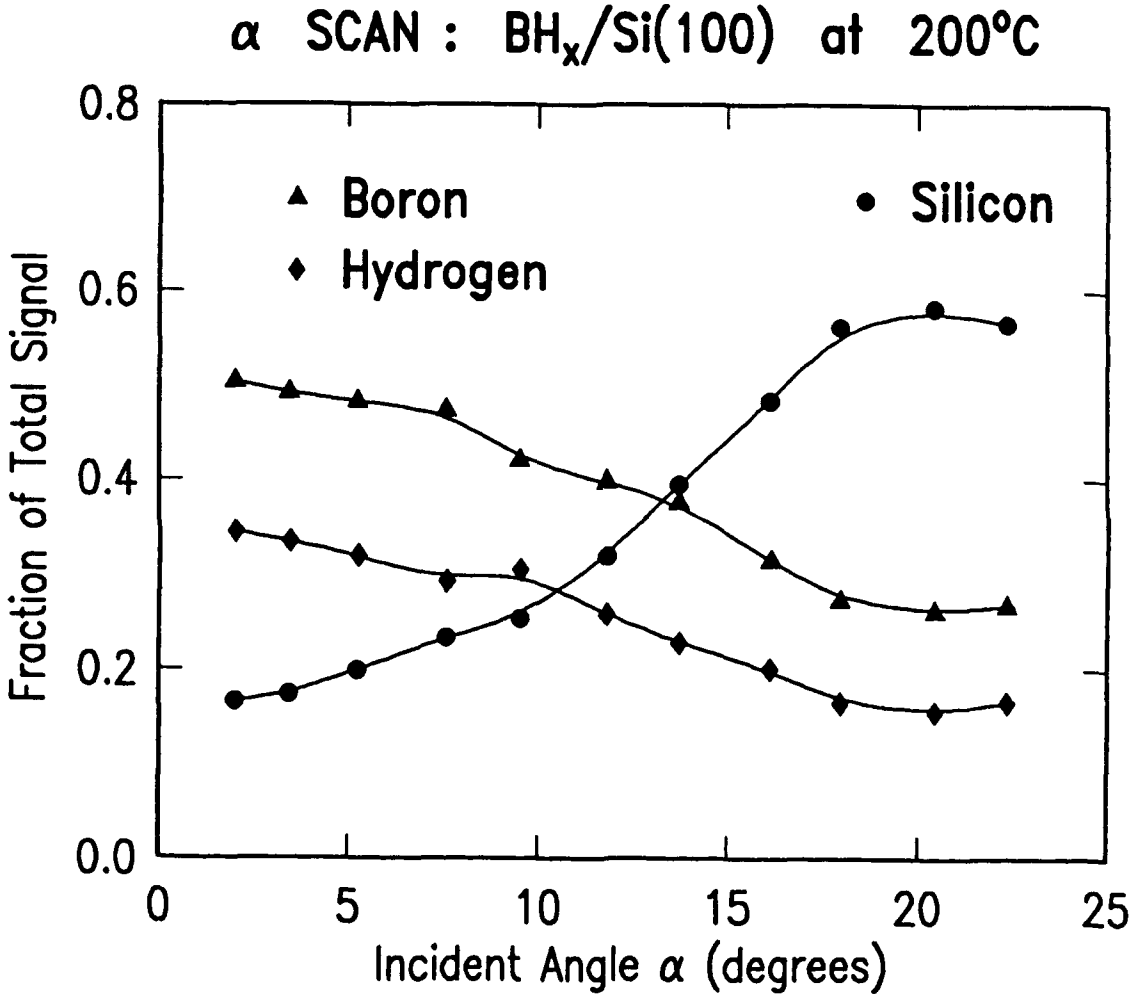
α SCAN : BHx/Si(100) at 200°C
Boron
Silicon
Hydrogen
Fraction of Total Signal
0.0
0.2
0.4
0.6
0.8
0
5
10
15
20
25
Incident Angle α (degrees)

Fig. 8

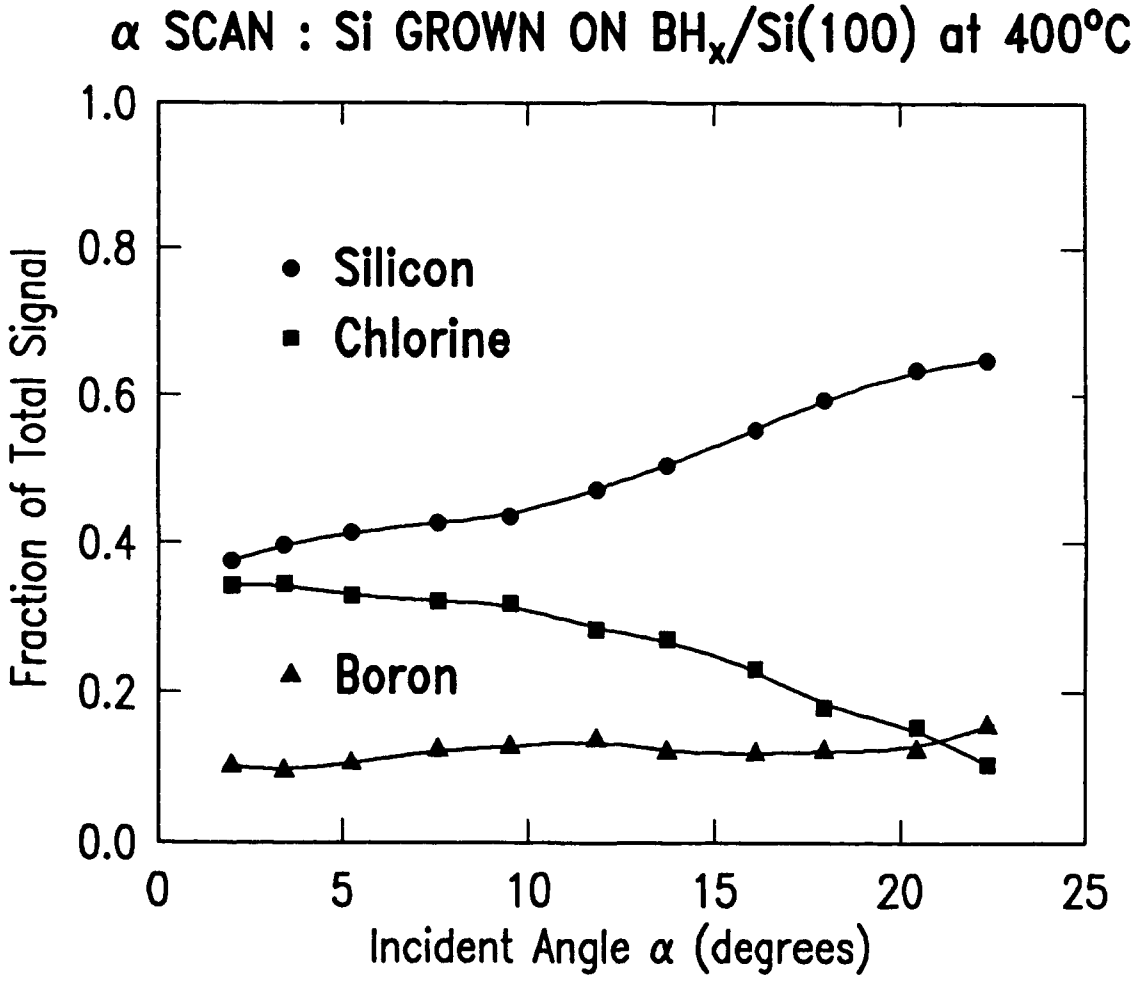
α SCAN : Si GROWN ON BHx/Si(100) at 400°C
Fraction of Total Signal
1.0
0.8
0.6
0.4
0.2
0.0
Silicon
Chlorine
Boron
0
5
10
15
20
25
Incident Angle α (degrees)

Appendix B

Appl. Phys. Lett.,
submitted ACCEPTED
Revised 4/24/92

ELEMENTAL MARKING OF Si ON Si(100) INTERFACES

S. M. Gates and D. D. Koleske

IBM T. J. Watson Research Center, Yorktown Hts., NY 10598

ABSTRACT

Submonolayer coverages of B, Sn and Ge are prepared on Si(100) surfaces, and characterized using time-of-flight Scattering and Recoiling Spectroscopy (TOF SARS). The dopant "marks" the initial Si interface, and Si is grown on top of the "marked" surface, and is designated Si* *Attenuation* of the elemental B, Sn and Ge signals by Si* is used to evaluate Si precursors for Atomic Layer Epitaxy (ALE), and compare the thermal stability of Si*/B/Si(100), Si*/Sn/Si(100) and Si*/Ge/Si(100) structures.

PACS numbers : 68.55.Ln , 68.35.Dv , 81.15.Gh , 82.65.Yh

The growth of II-VI and III-V semiconductor films in a self-limiting, layer-by-layer process at low temperature (T) is known as Atomic Layer Epitaxy (ALE) {1}. Concerning the ALE deposition of Si, recent growth {2,3} and surface chemistry {4-6} studies report submonolayer Si deposition from a saturation exposure of precursor gas. Coverages of Si (θ_{Si}) of 0.43 monolayer (ML) from Si_2H_6 {2}, and 0.5 ML from SiH_2Cl_2 {4} are found on Si(100), and methods to measure θ_{Si} are desired. In this letter, a submonolayer coverage of boron (B), tin (Sn) or germanium (Ge) is characterized by time-of-flight Scattering and Recoiling Spectroscopy (TOF-SARS), and this dopant "marks" the initial Si surface. After adsorption of a Si precursor at low T, *attenuation* of the TOF-SARS signals from the "marker" is used to monitor Si growth. We designate new Si grown atop the "marker" as Si^*. The preparation and thermal stability Si^*/B/Si(100), Si^*/Sn/Si(100) and Si^*/Ge/Si(100) structures is studied here with *in situ* analysis.

Using 1-5 keV ions, both the scattered primary ions and recoiled surface atoms provide surface composition and structure information. A pulsed primary ion beam (potassium in this work), and time-of-flight (TOF) detection are characteristic of TOF-SARS as reviewed by Rabalais {7,8}. Both scattered K^+ (a sensitive probe of heavy elements), and direct recoil (DR) particles are detected. From clean Si, the DR particles are predominantly neutral {9} while the K^+ remain charged. The neutrals and ions are separated when a grid located near the detector is biased positively to reject the K^+, as shown below and elsewhere {9,10}. Angles of incidence (α) of 3-5° with respect to the surface plane enhance surface sensitivity {10}. Data are signal averaged for 4 minutes using a pulsed K^+ current of 0.04 nA, giving a K^+ dose of $\simeq 10^{-3}$ ML per spectrum, or less than 0.01 ML during a series of 4-5 measurements.

We find that boron "markers" are stable to higher T than Sn or Ge. Figure 1 shows growth of a structure designated $Si^*/B/Si(100)$, with the detector grid biassed at +4 kV. Spectrum 1A shows the clean Si(100) surface and 1B shows the surface dosed to saturation with decaborane, $B_{10}H_{14}$, ($2x10^{16}$ cm.$^{-2}$) at 200°C, and heated to 650°C to desorb the H and to allow the B atoms to occupy a stable site, which may be subsurface. The B site location on Si(100) after annealling is unknown. Delta doped B layers of 1/2 ML are electrically active on Si(100) {11}, and on Si(111) the stable site for B is in the 3rd atomic layer substituted for a Si {12}. This B marked surface was then cooled to 300°C, dosed with $1x10^{19}$ Si_2Cl_6 cm.$^{-2}$, and spectrum 1C was taken. After Si_2Cl_6 dosing, the direct recoil B intensity (B_{DR}) in 1C is 0.67 times that in 1B. The original "marker" B_{DR} intensity has been attenuated by 33 % due to adsorption of Si^*. Following annealling to 450 and 500°C, respectively, spectra 1D and 1E were taken.

At 300°C, surface $SiCl_3$ and $SiCl_2$ groups are unstable and Si_2Cl_6 adsorption results in only SiCl species as seen by soft X-ray photoemission {13}. Saturation with Si_2Cl_6 should produce 1 ML of Cl, and adsorb 2/6 = 1/3 ML of Si^*. In Fig. 1, we see 33 % attenuation, and 4 repetitions of this experiment gave B signal attenuation by an average of 34 % with a range of 33-36 %. We conclude that use of TOF-SARS and B attenuation to measure Si^* coverage can be quantitative when chlorinated precursors are used. The $Si^*/B/Si(100)$ structure is completely stable at 450°C (spectrum 1D). Beginning at 500°C, Si^* is removed by thermal desorption of $SiCl_2$ {13}, increasing the B_{DR} signal.

When Si hydride precursors are used, the intense H direct recoil signal overlaps the B_{DR} signal, and the latter cannot be quantified accurately. A heavier "marker" element with a large time of flight would be desirable. Tin is considered in Figure 2, again using the biassed detector grid. Spectrum 2A shows the clean surface containing a trace of hydrogen. Spectrum 2B is from a surface dosed to saturation at 250°C with

tetraethyltin, $Sn(C_2H_5)_4$, and then heated to 650°C to desorb the ethyl groups. Some surface carbon and a well-resolved Sn recoil signal are seen. This surface was then cooled to 250°C and dosed with $2x10^{19}$ Si_2H_6 $cm.^{-2}$ (see spectrum 2C). Note that the Sn(DR) signal is attenuated in 2C. Using a flat background subtraction (2A), the Sn(DR) signal in 2C is 0.41 times of that in 2B. The original Sn marker signal is attenuated by 60 %, indicating that $\simeq$ 0.6 ML of Si^* was grown. The Si^*/Sn/Si(100) structure is metastable, as seen in spectrum 2D after heating to 460°C. In 2D, the Sn recoil signal has returned to its original level, concurrent with desorption of the surface H.

Another high mass "marker", Ge, is studied in Figure 3 and both scattered K^+ ions and DR particles are used (detector grid not biassed). In spectrum 3A from the clean surface, the feature at 7.8 μs is recoiled Si atoms (Si_{DR}), and the broad feature from 8-11 μs is due to K^+ scattered from Si in the 1st and 2nd layers ($K^+ \rightarrow Si$). In 3B, approximately 1/3 ML of Ge was added by GeH_4 adsorption at 500°C (the hydrogen desorbs at this T). The Ge coverage was determined assuming that a saturation Ge coverage from GeH_4 at 100°C equals 1/4 ML. The intense peak at 8.1 μs is K^+ scattered from Ge ($K^+ \rightarrow$ Ge) and the weak feature at 13.0 μs is recoiled Ge atoms (Ge_{DR}), shown amplified 10 times. Following spectrum 3B at 500°C, the sample was cooled to 300°C and dosed with $5x10^{19}$ Si_3H_8 $cm.^{-2}$, then spectrum 3C was taken. In 3C, both the Ge_{DR} and $K^+ \rightarrow$Ge features are significantly attenuated. The $K^+ \rightarrow$Ge signal overlaps with the Si_{DR} signal prohibiting quantitative use of the intense and surface specific $K^+ \rightarrow$Ge peak, so we use the Ge_{DR} signal. The inset in fig. 3 shows the fraction of the initial Ge_{DR} signal versus Si^* coverage, for a range of Si_3H_8 exposures. The H_{DR} peak height was calibrated, and Si^* coverage was computed using the 8/3 H/Si ratio in Si_3H_8. This plot provides a calibration for measurement of Si^* coverage using attenuation of the Ge_{DR} peak height. The plot is approximately linear up to 0.2 ML Si^* coverage, and curves from 0.2 to 0.33 ML of Si^*.

The Si^*/Ge/Si(100) structure is metastable. Raising the temperature to 400°C (3D) causes desorption of H as H_2 and concurrent Ge segregation to surface sites on top of the Si^*. Both the Ge_{DR} and $K^+ \rightarrow Ge$ features return to their original levels. Migration of the Ge marker is about 90% complete after 2 minutes at 400°C (3D), and complete at 550°C (not shown). The segregation of dopants during MBE Si growth is well known {14}, and can be suppressed using arsenic or antimony as a "surfactant" {15}. The data of fig. 3 demonstrate that termination of the surface dangling bonds with H prevents Ge segregation, for temperatures below the H_2 desorption threshold. Termination of the dangling bonds with As or Sb has a similar effect at 500°C {15}.

In summary, attenuation of direct recoil signals from the "marker" elements B, Sn and Ge can be used to study the self-limiting adsorption step in Si atomic layer epitaxy. The Si^*/B/Si(100) structures are stable at 450°C. The related Si^*/Sn/Si(100) and Si^*/Ge/Si(100) structures are only stable provided the Si^* surface is terminated with hydrogen. These 2 structures decompose below 400°C by dopant segregation to the surface when the surface dangling bonds are not blocked with hydrogen.

Acknowledgement

This work is supported by the Office of Naval Research under contract # N00014-91-C-0080.

REFERENCES

1. T. Suntola and M. Simpson (Eds.); "Atomic Layer Epitaxy", Chapman and Hall, NY, NY; copyright 1990 by Blackie & Son, Ltd., London.
2. D. Lubben, R. Tsu, T.R. Bramblett and J.E. Greene, J. Vac. Sci. Tech. **A 9**, 3003 (1991).
3. J. Nishizawa, K. Aoki, S. Suzuki and K. Kikuchi, J. Crystal Growth **99**, 502 (1990).
4. J.A. Yarmoff, D.K. Shuh, T.D. Durbin, C.W. Lo, D.A. Lapiano-Smith, F.R. McFeely and F.J. Himpsel; J. Vac. Sci. Tech., submitted.
5. Y. Takahashi and T. Urisu; Jap. J. Appl. Phys. **30**, L209 (1991).
6. P.A. Coon, P. Gupta, M.L. Wise and S.M. George; J. Vac. Sci. Tech. A **10**, 324 (1992).
7. J.W. Rabalais; Science **250**, 522 (1990).
8. J.W. Rabalais, CRC Crit. Rev. Solid State Mater. Sci. **14**, 319 (1988).
9. S.M. Gates and S.K.Kulkarni; Appl. Phys. Lett. **60**, 53 (1992).
10. S.M. Gates, C.-M. Chiang and D.B. Beach; J. Appl. Phys., in press.
11. R.L. Headrick, B.E. Weir, A.F.J. Levi, D.J. Eaglesham and L.C. Feldman; Appl. Phys. Lett.**57**, 2779 (1990).
12. I.W. Lyo, E. Kaxiras and Ph. Avouris; Phys. Rev. Lett. **63**, 1261 (1989). Ph. Avouris, I.W. Lyo, F. Bozso and E. Kaxiras; J. Vac. Sci. Tech. **A8**, 3405 (1990).
13. L.J. Whitman, S.A. Joyce, J.A. Yarmoff, F.R. McFeely and L.J. Terminello; Surf. Sci. **232**, 297 (1990).
14. K. Nakagawa, M. Miyao, and Y. Shiraki; Thin Solid Films, **183**, 315 (1989).
15. M. Copel, M.C. Reuter, M. Horn von Hoegen and R.M. Tromp; Phys. Rev. B **42**, 11682 (1990).

FIGURE CAPTIONS

FIGURE 1. Tof-SARS spectra using 4 keV potassium ions (K^+), 5° angle of incidence with respect to the surface plane, and the detector grid at + 4 kV. A: clean Si(100)-(2X1), B: dosed with $2x10^{16}$ cm.$^{-2}$ $B_{10}H_{14}$ at 200°C, at 300°C and then heated to 650°C. In C, $1x10^{19}$ Si_2Cl_6 cm.$^{-2}$ was dosed at 300°C. In D and E, this surface is heated to the indicated temperature (T) for 4 minutes at each T.

FIGURE 2. Tof-SARS spectra with the same conditions as Figure 1. A: clean Si(100)-(2X1), B: $3x10^{16}$ cm.$^{-2}$ tetraethyltin, $Sn(C_2H_5)_4$, dosed at 250°C and then heated to 650°C. In C, $1x10^{19}$ Si_2H_6 cm.$^{-2}$ was dosed at 250°C. In D, this surface is heated to 450°C for 4 minutes.

FIGURE 3. Tof-SARS spectra using 4 keV potassium ions (K^+), 3° angle of incidence with respect to the surface plane, and the detector grid at ground potential. A: clean Si(100)-(2X1), B: $9x10^{17}$ GeH_4 cm.$^{-2}$ dosed at 500°C. In C, $1x10^{19}$ Si_3H_8 cm.$^{-2}$ was dosed at 300°C. In D, the surface from C was heated to 400°C. The inset is described in the text.

Fig. 1

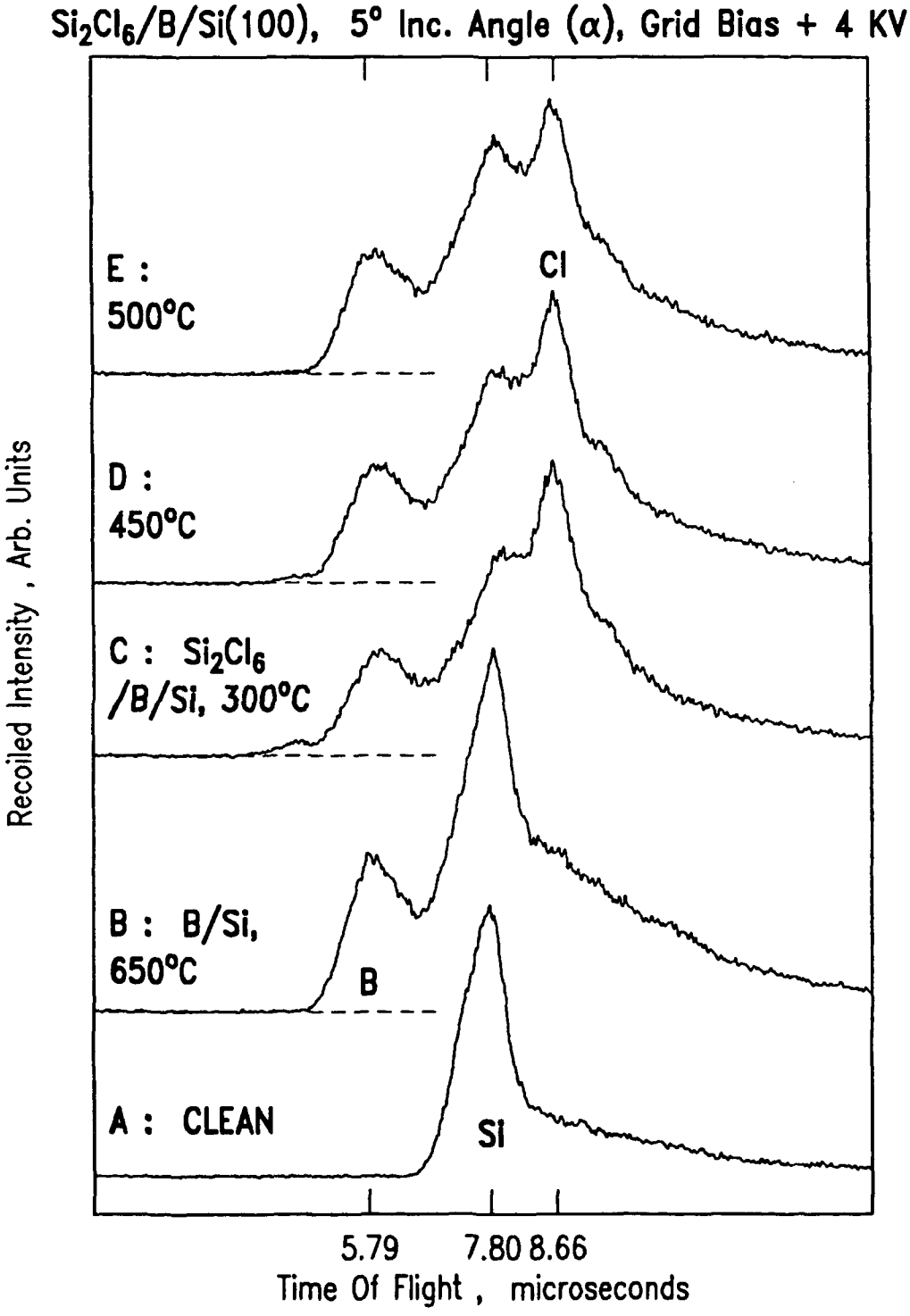
Si_2Cl_6/B/Si(100), 5° Inc. Angle (α), Grid Bias + 4 KV
E : 500°C
Cl
D : 450°C
C : Si_2Cl_6 /B/Si, 300°C
B : B/Si, 650°C
B
A : CLEAN
Si
Recoiled Intensity , Arb. Units
5.79
7.80
8.66
Time Of Flight , microseconds

Fig. 2

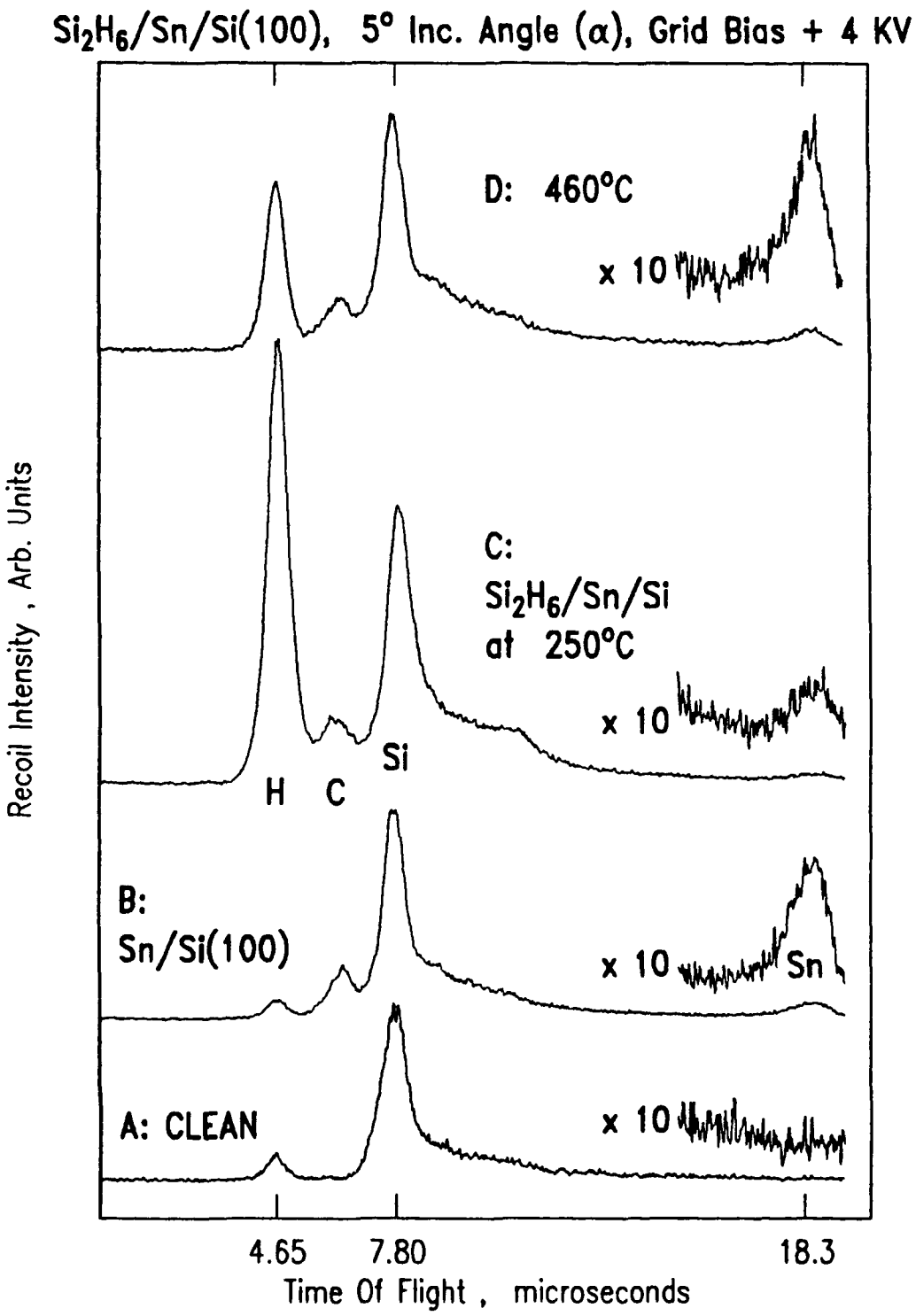
Si_2H_6/Sn/Si(100), 5° Inc. Angle (α), Grid Bias + 4 KV
D: 460°C
x 10
C:
Si_2H_6/Sn/Si
at 250°C
x 10
H
C
Si
B:
Sn/Si(100)
x 10
Sn
A: CLEAN
x 10
Recoil Intensity , Arb. Units
4.65
7.80
18.3
Time Of Flight , microseconds

Fig. 3

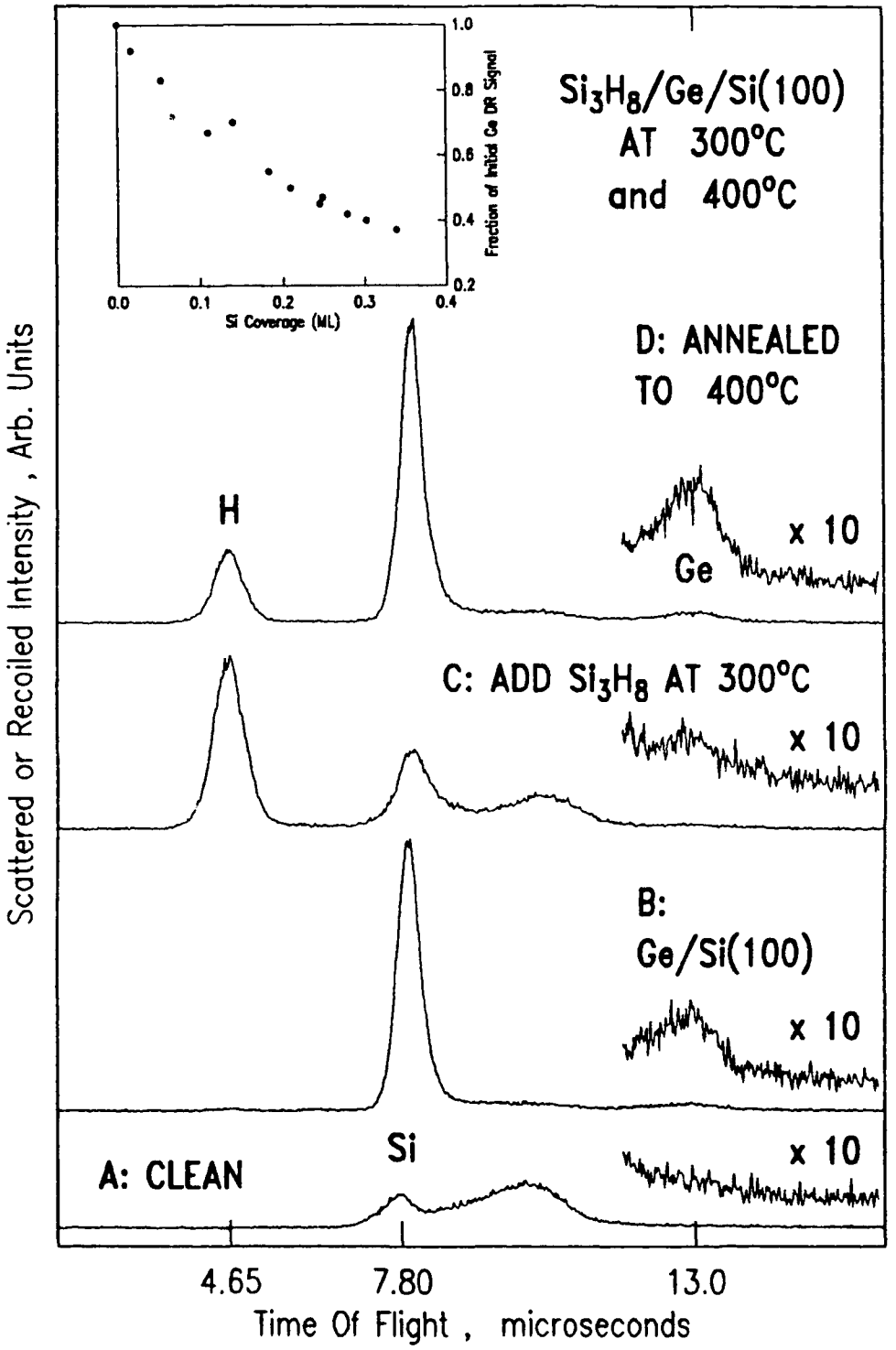
Si3H8/Ge/Si(100)
AT 300°C
and 400°C
D: ANNEALED
TO 400°C
H
Ge
x 10
C: ADD Si3H8 AT 300°C
x 10
B:
Ge/Si(100)
x 10
A: CLEAN
Si
x 10
Scattered or Recoiled Intensity , Arb. Units
4.65
7.80
13.0
Time Of Flight , microseconds
Si Coverage (ML)
Fraction of Initial Ge DR Signal
0.0
0.1
0.2
0.3
0.4
0.2
0.4
0.6
0.8
1.0